Chemistry of Metal and Semimetal Cluster Ions

Denise C. Parent*

Chemistry Division/Code 6113, Naval Research Laboratory, Washington, D.C. 20375-5000

Scott L. Anderson*

Department of Chemistry, State University of New York at Stony Brook, Stony Brook, New York 11794-3400

Received May 15, 1992 (Revised Manuscript Received August 13, 1992)

Contents

Denise Parent was born in Sherbrooke, Quebec, Canada, and raised in California. She received both her B.A. (1977) and Ph.D. (1983) in Chemistry at the University of California at Santa Barbara. Her postdoctoral work included sojourns in Orsay on a NATO Fellowship and at Los Alamos National Laboratory. She joined the Naval Research Laboratory as a staff member in 1987, where she has concentrated on studies of ion cluster chemistry. Her other professional interests include the ion chemistry of interstellar and planetary atmospheres, energy effects and energy deposition in ion–molecule reactions, and the ion chemistry relevant to materials processing. Spare time pursuits include travel, needlework, and photography.

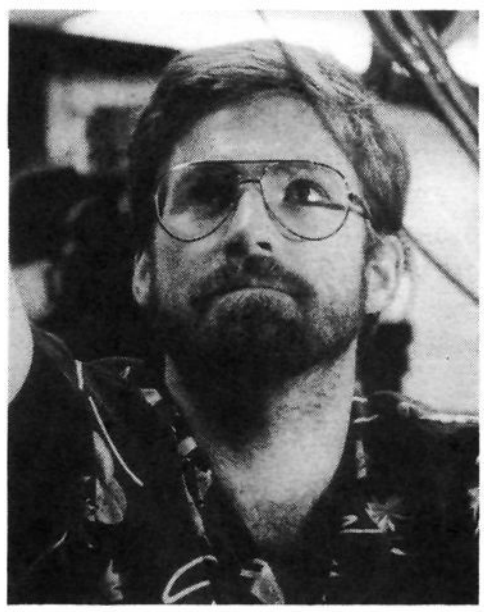

Scott Anderson was born in Wilmington, DE, and raised all over the United States. He received a B.A. from Rice University (1977) and a Ph.D. from the University of California at Berkeley (1981). After postdoctoral research at Stanford University, he joined the Chemistry Department of the State University of New York at Stony Brook. Anderson's current research activities are in the areas of cluster ion chemistry, state-selected ion reaction dynamics, site-selective X-ray photochemistry in solids, and multiphoton spectroscopy. He enjoys windsurfing, mountain biking, and other violent physical activities.

I. Introduction

The explosion of growth in cluster research during the past 10 years has been phenomenal. In this article, we will attempt to give a reasonably comprehensive survey of a small subset of the cluster field—gas-phase chemistry of metal and semimetal cluster ions. Even after focusing our attention on this subset, we are unable to present a thorough review of all studies. Rather, we will attempt to give a broad overview, using more detailed discussions of selected systems to illustrate some of the problems and opportunities currently existing.

The scope of this article encompasses atomic cluster ions composed of metallic and semimetallic elements. In addition to pure elemental clusters, mixed-metal clusters and clusters containing other elements such as

0009-2665/92/0792-1541$10.00/0

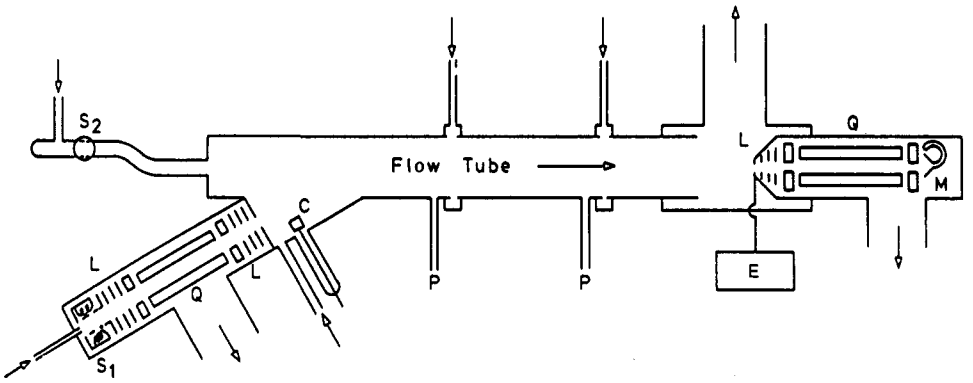

Figure 1. Schematic diagram of a SIFT apparatus with two ion sources: S_1 is an electron impact source with ion selection and S_2 is a microwave discharge source without ion selection which allows the apparatus to operate as a flowing afterglow. The arrows indicate the direction of gas flow. Various components are indicated by the following letters: L, electrostatic lenses; Q, quadrupole mass filters; C, ion collector; P, pressure measurement ports; E, electrometer; M, channel multiplier. (Adapted and reprinted from ref 10. Copyright 1979 Academic Press.)

N, O, and S will also be covered. Greater emphasis will be placed on the clusters of main group metals than on the transition metal clusters. This is mainly due to the concentration of results, from many different experimental and theoretical research groups, on clusters of several main group elements. This allows systematic comparisons between different classes of reactions and helps in elucidating the effects of cluster structure on chemistry. In addition, the authors' area of interest to date has been on main group clusters. We will focus our coverage on gas-phase chemistry with references to low-energy collision-induced dissociation (CID) and theoretical results when relevant. The review covers the period from 1988 to early 1992. There are a number of previous reviews[1-4] which have included metal and semimetal cluster ion chemistry up to 1988. There are also many conference proceedings and journal issues devoted to the general field of clusters.

This review will emphasize the relationship between structure and chemistry. Specifically we will ask the question: "What does chemistry reveal about structure?" In addition, a review of this type allows us to make comparisons among clusters of different elements.

Some specific areas of research, while falling within the domain of this review, have had to be deemphasized or excluded. These include work on ligated clusters, measurements of ionization potentials and electron affinities by chemical reactions, and work on fullerenes. The latter domain has become very active in the last two years, and we will not attempt to cover it. Two reviews that specifically discuss the gas-phase chemistry of these compounds have recently appeared.[5,6]

II. Techniques for the Study of Cluster Ion Chemistry

In this section, the major techniques used in studies of cluster ion chemistry will be discussed. These are high-pressure flow kinetics methods, Fourier transform ion cyclotron resonance mass spectrometry, and ion beam scattering, at both low and high collision energies. All are well implanted in the general ion chemistry community, and the generic methodology has been fully described in the literature. Brief descriptions and references will be given for each instrument type. The emphasis here will be on aspects specific to cluster studies, on the advantages and disadvantages of the various techniques for cluster studies, and on recent improvements that have had an impact on cluster studies.

Development of a variety of sources to interface with the instruments listed above has been the most effectual factor in fueling the growth in cluster ion studies. In the last part of this section we will describe the various sources used in the study of cluster ion *chemistry*, and in particular discuss the question of energy content of the cluster ions. This is a controversial area, as will be seen in the discussion of results.

A. High-Pressure Systems

Various flow reactors, such as flow-drift tubes and selected-ion flow tubes (SIFT), have been extensively used to study ion–molecule chemistry since their development in the 1960s and 1970s.[7-10] Ions are produced in an ion source and injected into the bulk flow. In SIFT[9,10] experiments the reactant ions are mass selected before they encounter the neutral reactant. This feature is particularly desirable in cluster ion studies, since many reactions may result in fragmentation of the cluster, and thus in ambiguities in assigning products to particular size reactants. Unfortunately, much of the cluster ion flow reactor work has not used SIFT and is thus somewhat difficult to interpret. After injection, the ions drift or flow down the tube in a carrier gas and react with neutral reagents introduced into the carrier gas downstream from the ion source. In drift tubes an electric field is applied in the flow direction, to "drift" the ions along the reactor. This allows one to vary the relative translational and internal energies of the ions. However, only an effective temperature can be defined since the distribution of velocities is non-Maxwellian. At the end of the reactor, the ion population is sampled through a small orifice into a mass spectrometer, where the ions are mass identified and counted. Discrimination in sampling, including fragmentation, must be avoided to obtain accurate product ratios and rate constants. Figure 1 is a schematic diagram of a hybrid flow-drift tube with a selected-ion source.

A related instrument type uses an ion beam instrument to inject cluster ions into a high-pressure, variable-

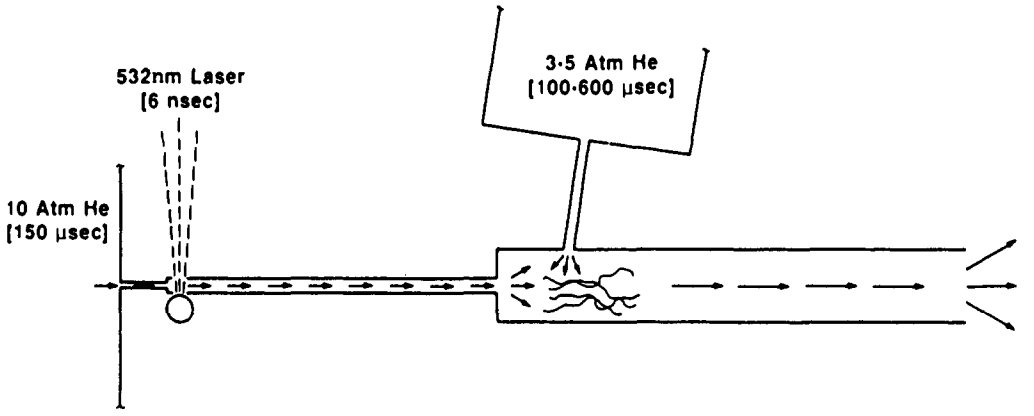

Figure 2. Simplified schematic of the fast-flow reactor showing the source and reactor regions. From left to right the essential features are the high-pressure stagnation chamber and pulsed nozzle, the target rod and vaporization laser, the 2-mm condensation channel which opens into the 1.1-cm-diameter reactor (where the diluted neutral reactant is introduced with a second pulsed nozzle), and the expansion into the detection region (not shown). (Adapted and reprinted from ref 14. Copyright 1985 American Chemical Society.)

temperature drift cell. Bowers and colleagues[11] have built an instrument based on a commercial high-resolution mass spectrometer. A cluster ion source is attached to a VG ZAB-2F reverse-geometry mass spectrometer, and the resulting mass-selected 5-keV ion beam is decelerated to between 0–10 eV and focused into a conventional drift cell. Reaction rate constants and ion mobilities can be measured. Jarrold and co-workers[12] have achieved similar results, modifying a low-energy cluster ion beam instrument (described in section II.C) by simply replacing the low-pressure scattering cell with a high-pressure drift cell. This instrument uses quadrupole mass filters.

In high-pressure flow instruments, pseudo-first-order kinetics as given by eq 1 are usually observed. I_0 and

$$\ln (I/I_0) = -kNt \qquad (1)$$

I are the initial and final reactant ion intensities, k is the bimolecular rate constant, N is the neutral reactant concentration, and t is the reaction time. Either t or N can be varied and both parameters need to be measured to obtain absolute values of k. Because the total pressure is typically 0.1–1 Torr, three-body processes are also possible, leading to stabilization of products such as adducts.

The fast-flow reactor, normally used for the study of neutral species including clusters,[13,14,15] has also been utilized to a lesser extent for cluster ion chemistry experiments. A schematic diagram of the fast flow reactor is given in Figure 2. Clusters are formed in a long, narrow channel and are swept by a high-pressure pulse of He gas into the reactor (total pressure $\approx$ 60 Torr) where they intersect a pulse of reactant neutral gas. In essence, these reactors are simply a type of laser vaporization source (see section II.D.3), with a downstream inlet for the reactant gas. The reaction zone extends to the end of the reactor where the gas expands into vacuum and is sampled by mass spectrometry. Relative reactivities are determined by measuring the ratio of product ions to initial reactant.

In contrast to most techniques currently used for cluster studies, there is no mass selection of the reactant ion in the fast-flow reactor. All ions produced by the source are expanded into the reactor and detected. Thus any fragmentation of clusters to smaller clusters may not be noticeable. In addition, neutral species and clusters are also present in the source and reactor, thus posing the possibility of charge exchange between the ionic and neutral clusters. However, Zakin et al.[16,17] observed no effect on the ion or neutral cluster reactivity patterns when the diameter of the reactor was increased by 3.3 (thus decreasing the gas density and charge transfer probability by a factor of >10). This was interpreted as indicating that interaction between the two sets of clusters is minimal. An additional question, as in all experiments, is that of reactant cluster internal temperature. The section on laser vaporization sources includes some discussion of this issue.

B. Fourier Transform Ion Cyclotron Resonance Mass Spectrometry

The techniques of ion cyclotron resonance (ICR) mass spectrometry and its offspring, Fourier transform ion cyclotron resonance (FT-ICR) mass spectrometry (also frequently referred to as FTMS by the analytically minded), have been widely reviewed.[18–24] Very briefly, ions are trapped in a "cell" by magnetic and electric fields, shown schematically in Figure 3. Ions of a particular mass-to-charge ratio m/z orbit about the magnetic field vector with a characteristic cyclotron frequency ω which depends on the magnetic field strength and m/z but not on the ion velocity. Mass selection, ion excitation, and ion detection all rely on this property of ICR, through application of an electric field at the appropriate frequency on the excitation plates. Whether ions are simply kinetically excited, or are "ejected" from the cell, depends on the magnitude and duration of the electric field applied. The depth of the trapping potential created by the electric field, typically 2 V, provides a rough upper limit to the kinetic energy of the trapped ions. In contrast to the older ICR technique, FT-ICR allows ions of all m/z to be detected at once. When detecting ions over a large mass range, common in cluster work, care to avoid mass discrimination is needed.

Ions can either be formed in situ and trapped or can be produced in an external source and injected into the cell. Ion–molecule reactions and other processes are studied under low-pressure conditions (typically much less than 10^{-5} Torr), thus three-body collisions are

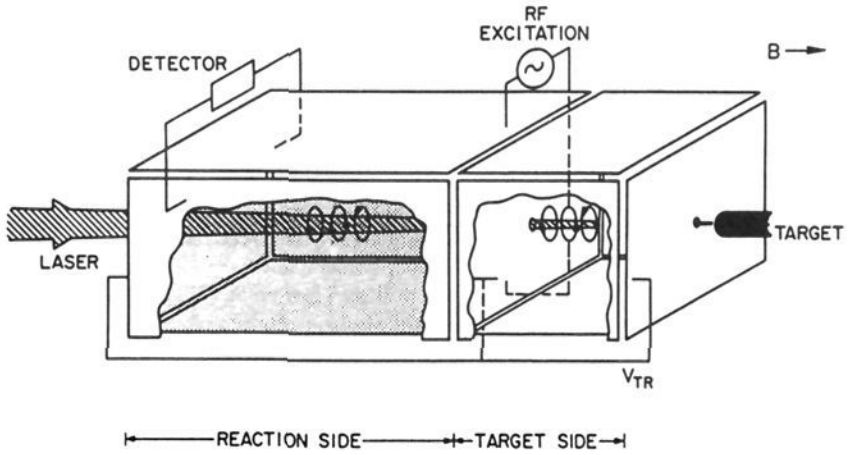

Figure 3. Schematic diagram of a dual ICR cell, showing the magnetic field vector B and ion formation by laser vaporization of a solid target placed external to the cell. Ions can also be produced by electron impact or injected into the cell from an external source. The cyclotron motion of the ions around the magnetic field vector is also indicated. Application of a potential V_{TR} on the plates perpendicular to B serve to trap the ions in the direction of the magnetic field. Excitation and detection of the ions is achieved by applying a radio frequency field to one set of opposing plates and detecting on the other set. A single-cell configuration consists of the reaction side only. (Adapted and reprinted from Mandich, M. L.; Bondybey, V. E.; Reents, W. D., Jr. *J. Chem. Phys.* **1987**, *86*, 4245. Copyright 1987 American Institute of Physics.)

unimportant. Bimolecular reaction rate constants are determined by varying the reaction time and monitoring the pseudo-first-order kinetics given by eq 1. In order to obtain absolute rate constants the neutral reactant concentration must be determined, which usually means calibrating the pressure of the neutral by reference to known reactions. This procedure typically introduces the largest source of error in the reported rate constants. The ions can be trapped for long periods of time to undergo multiple collisions, which permits the study of slow processes. Rate constants as small as 1×10^{-14} cm^3/s can be measured under the best conditions. One unique aspect of ICR techniques is that time, not space, is the important variable. All phases of the experiment, from ion production through selection, reaction, and detection, can be carried out in the cell through the use of pulses to initiate the different events. The ICR technique is also capable of performing MS^n (tandem mass spectrometry) expriments, with n being limited by the trapping efficiency and possibly the software. Multiple MS sequences can be used to elucidate reaction pathways, study sequential reactions, and perform low-energy collision-induced dissociation (CID) on reaction products.

Recent developments in FT-ICR which have had the most impact on the cluster field are the use of different types of external sources, discussed in detail in section II.D, and the implementation of SWIFT (stored waveform inverse Fourier transform). SWIFT, developed by Marshall and co-workers[25] is a method to precisely excite and eject ions of selected m/z values without exciting ions at other m/z values (and thus increasing their kinetic and/or internal energy), which can easily occur using conventional methods. Smalley and co-workers[26] have fully described various aspects of the SWIFT technique and its implementation on their FT-ICR instrument. Figure 4 is a vivid example of the power and utility of the SWIFT technique.

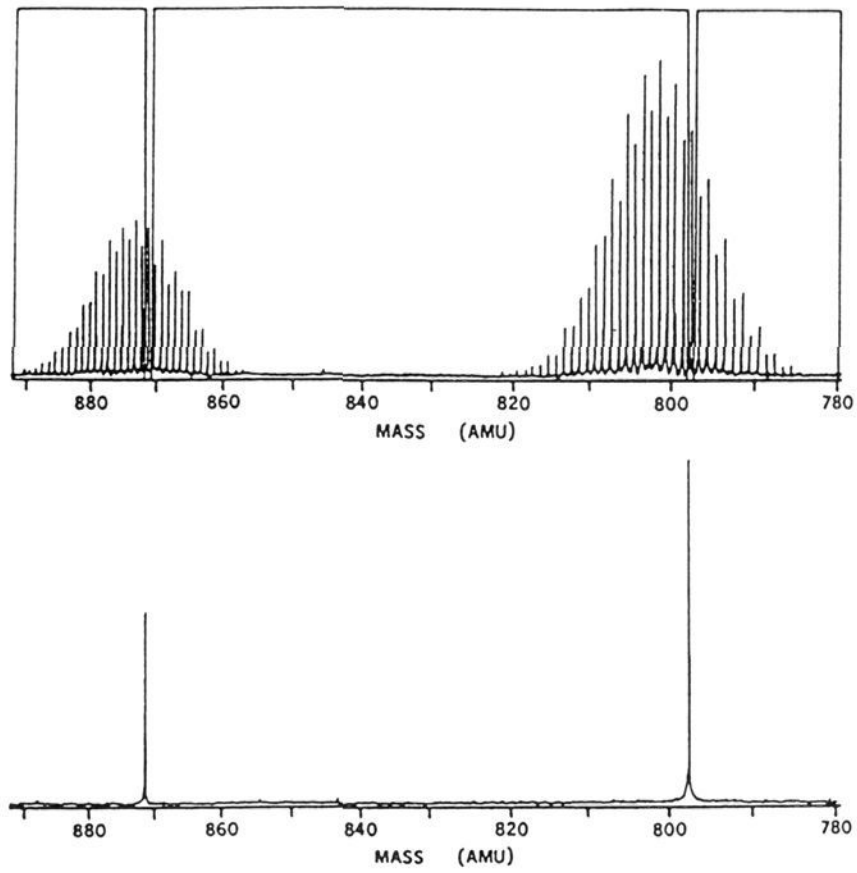

Figure 4. Two FT-ICR spectra demonstrating the use of SWIFT. In the top panel the broad isotopomer distributions for Ge_{11}^+ and Ge_{12}^+ are shown. The triple block SWIFT excitation also shown in the top panel was used to select a single isotopic peak out of each distribution, seen in the bottom panel. (Adapted and reprinted from ref 26. Copyright 1991 American Institute of Physics.)

C. Ion Beams

Ion beam scattering experiments allow study of cluster ion reactions over a wide range of collision energies. These results provide thermochemical data and mechanistic insight, which complement the thermal energy kinetic results from high-pressure and ICR techniques. A variety of instrument types have been used, ranging from those specially designed for cluster work to commercial mass spectrometers. The general features of ion beam chemistry instrumentation have been reviewed by Futrell[27] and Farrar.[28] In most beam experiments, the basic operating principles are similar. An ion source/mass filter combination is used to produce a monoenergetic beam of size-selected cluster ions. These are passed through a cloud of the neutral target molecule, and the product ions are collected, mass analyzed, and detected. The data consists of a set of intensity measurements for the reactant and all product ions, taken as a function of collision energy and reactant cluster size. Reaction cross sections are calculated from the ratio of the product and reactant intensities, and absolute cross sections can be obtained if the density times length product for the target gas is known.

There are several experimental issues which are particularly important or problematic in cluster ion chemistry work. Some provision should be made for dealing with internally hot reactant cluster ions (see section II.E). This is critical if accurate thermochemical data is to be extracted, and may even influence the perceived reaction mechanisms if the clusters are hot enough. For chemistry studies, it is useful to cover a center-of-mass collision energy range from several times the characteristic bond energies (10–20 eV) down to thermal (~0.05 eV). Since the reactant cluster mass is varied over a wide range, the lab frame kinetic energy

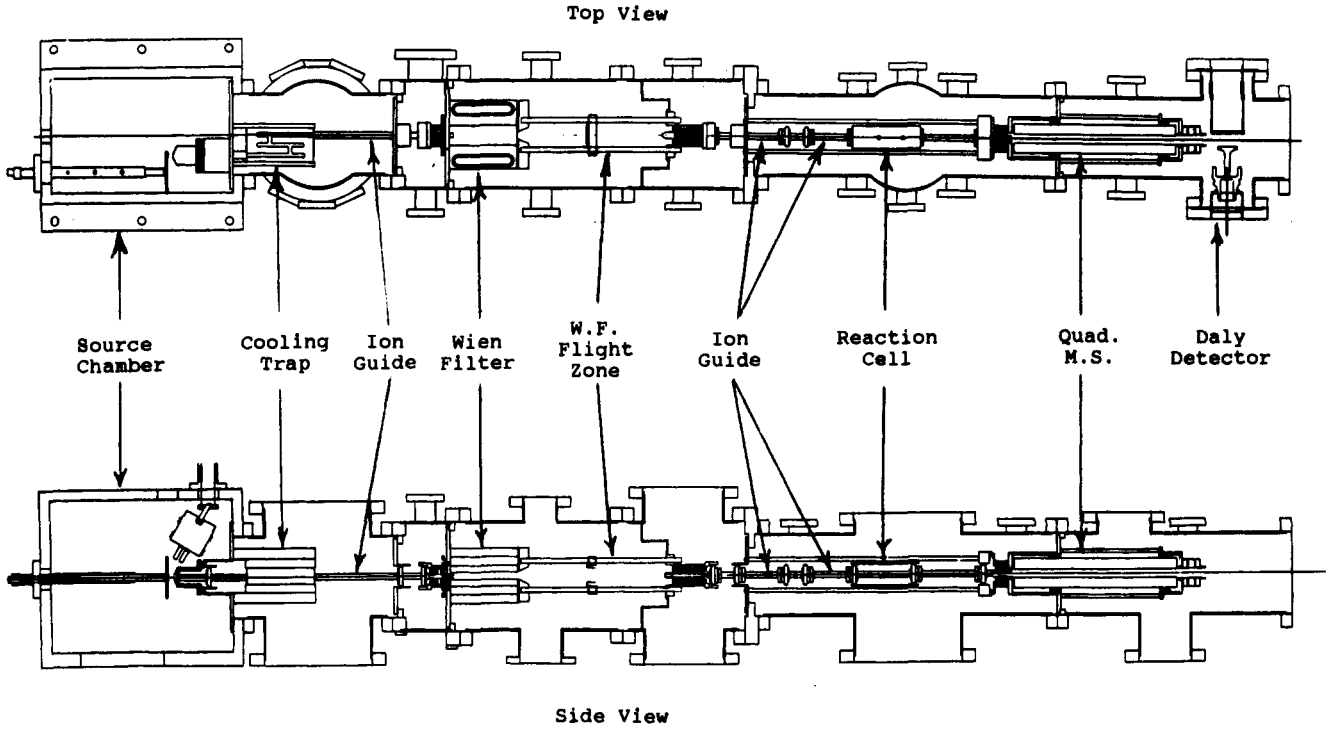

Figure 5. Schematic of one Stony Brook ion cluster beam machine. From left to right, ions are produced in a variety of sources (FAB is shown) and then trapped in a radio frequency labyrinth for cooling. A single cluster ion size is selected using a Wien filter, and then reactions are carried out in a octapole ion guide. Products are collected by the guide, mass analyzed with a quadrupole filter, and then counted by a Daly detector.

needs to be variable from hundreds of electronvolts down to ~100 meV. Cluster ion reactions may give product ions with very different masses and lab frame angular and energy distributions. Ion collection/detection efficiency must be independent of mass and scattering kinematics, otherwise the resulting distortions in product branching ratios and absolute cross sections may lead to incorrect conclusions about reaction mechanisms.

An issue that affects all types of experiments, but especially beam experiments, is the long time scales for cluster reactions. Consider the common case of cluster reactions proceeding through an activated intermediate complex:

$$M_x^+ + A \rightarrow M_xA^{+\dagger} \rightarrow M_{x-1}^+ + MA$$

In general, the lifetime of the $M_xA^{+\dagger}$ intermediate decreases with increasing available energy, and increases rapidly as the number of degrees of freedom increases. In order to observe the final M_{x-1}^+ product, the experiment must allow sufficient time between the initial collision and product detection. For low-energy collisions of cluster ions containing more than 20 atoms, intermediate lifetimes can range into the millisecond regime, while most beam experiments have time scales between ~10 and ~500 μs. This can result in substantial kinetic shifts in the observed energetics, i.e. no signal is observed for the M_{x-1}^+ product until the collision energy is great enough to decrease the $M_xA^{+\dagger}$ lifetime into the experimentally observable range. Hales et al.[29] have used RRKM unimolecular rate theory to correct experimental cross sections and extract threshold energies for collision-induced dissociation. This approach appears to be valuable as long as the magnitude of the kinetic shift is small. Note that for reactions of C_{60}^+, kinetic shifts of 20 eV are routinely observed on a millisecond experimental time scale;[30] clearly it is nontrivial to extract accurate thermochemical parameters for large cluster ions. As intermediate lifetimes increase beyond the 100-μs range, radiative stabilization begins to compete with product formation. This ultimately sets a limit on how accurately energetics can be determined for large clusters, regardless of the experimental time scale.

The most detailed cluster beam studies have used low energy ion beam instruments that were specially designed for cluster work. Figure 5 shows one machine at Stony Brook that is optimized for clusters containing up to ~15 atoms. This instrument has been described in detail,[31] and only the important features are summarized here. The instrument is equipped with both laser ablation (not shown) and sputtering sources, both of which produce hot reactant cluster ions. Storage in a radio frequency trap (see section II.E) is used to cool the clusters to room temperature, after which they are mass selected using a Wien filter. The cool, mass-selected ion beam is injected into a set of radio frequency ion guides[32] which pass the reactant clusters through a gas cell containing ~10^{-5} Torr of neutral reactant. The octapole ion guide collects product ions independent of scattering angle (within limits determined by product ion mass and recoil energy) and guides them to the final quadrupole mass spectrometer. A typical experiment consists of varying cluster size and collision energy while measuring absolute cross sections for all product ion channels.

Several other low-energy cluster ion beam instruments have been constructed, differing principally in the source and mass filter designs. Jarrold and coworkers[33] have combined a specially designed quasi-cw laser vaporization cluster ion source with a tandem quadrupole mass spectrometer, for study of beam and,

more recently, drift-cell reactions of clusters containing up to 70 atoms. Armentrout and co-workers[34] also have developed a cw laser vaporization cluster source, which is incorporated into a tandem mass spectrometer that uses a magnetic sector to mass select the reactant cluster ions and a quadrupole to analyze the products. Finally, at Stony Brook, we have a second cluster beam instrument which is designed for experiments with clusters containing up to 200 atoms.[35] Sputtering, laser ablation, or laser vaporization are used to produce cluster ions, which are cooled by storage in a buffer gas, then mass selected by a magnetic sector. To compensate for the wide range of product masses and laboratory kinetic energies possible in the reactions of large clusters, a double-focusing electric/magnetic sector mass filter serves as the product mass analyzer.

To date, all beam experiments on metal and semimetal cluster ions have either measured product ions that are forward scattered into the detector or have used ion guides to collect ions scattered at all angles. No true differential cross sections (i.e. measurements of product ion angular and energy distributions) have been obtained, although ion guide techniques have been used to obtain crude differential results for C_{60} reactive scattering.[30]

D. Ion Sources

We will only discuss cluster ion sources that have been used for chemistry studies; other types of sources also exist but will not be covered. From this perspective, there are two basic desiderata for sources. Obviously the source should produce a wide range of cluster ion sizes from nearly any starting material, preferably without excessive contaminants. Ideally, the source should also produce cluster ions which are internally cold, or at least in a known internal energy distribution. Unfortunately, except for small clusters which are amenable to spectroscopic probing, there is no direct way to measure cluster internal energy, and this chemically important parameter is usually not known. This section will discuss each type of source; the following section outlines methods for cooling hot cluster ions.

1. Direct Laser Vaporization

In the direct laser vaporization (DLV) source, a pulsed laser is used to vaporize a solid sample placed in high vacuum (<10^{-6} Torr). Material ejected from the sample expands directly into the vacuum without the presence of a buffer gas, and cluster ions are created directly in the vaporization process. DLV is especially compatible with high-vacuum techniques and is easily implemented in conjunction with FT-ICR, where the sample is placed just outside the cell, as shown in Figure 3. DLV has been used primarily to produce pure clusters of main group elements such as carbon and silicon.[36-38] Mixed clusters containing a metal and a nonmetal have also been produced by DLV of mixed samples or metal compounds.[39-43] The only large pure metal cluster ions that have been produced by DLV are of aluminum, using targets of aluminum[44] or aluminum nitride.[45] Thus the utility of the DLV technique is somewhat limited in the range of cluster ions that can be produced.

Since the DLV technique uses no buffer gas, the nascent cluster ions may have large internal energies.

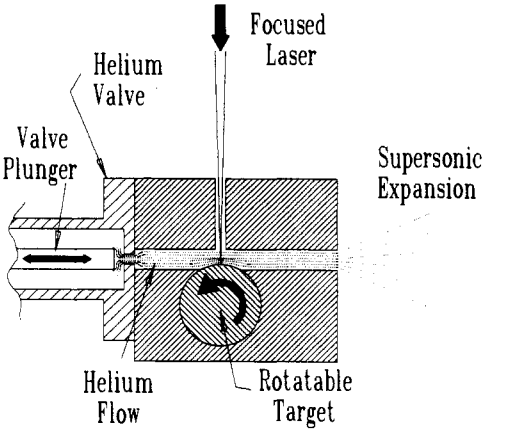

Figure 6. Schematic of a basic laser vaporization (LV) source. Helium buffer gas flows through the channel from left to right, passing over a target of the cluster precursor. The vaporization laser is focused onto the target, creating a hot plasma, which is confined and cooled by the buffer gas. Clusters form in the supersaturated vapor as it moves down the channel, and then exit in a supersonic expansion into the vacuum chamber. Many modifications are possible for different purposes, including pulsed or continuous flows; rod, disk, or "chunk" shaped targets; injection of electrons into the flow to enhance ionization; addition of various shaped extensions to the flow channel to enhance clustering or cooling; addition of flow tube reactors to the source exit for chemistry studies.

Somewhat surprisingly, most kinetic studies in the FT-ICR have not observed effects which could arise from excess energy in the ions. This may be due to the relatively long time (100 ms or more) used for mass selection before the kinetic measurements are begun. During this time the ions can relax by radiative decay. For specific ions, such as C_3^+, TaC_y^+ (y = 8, 9, 11), and $Si_2C_y^+$ ($y > 2$), nonlinear decay plots postulated to be due to internal energy have been observed.[46,47,48] Collisional cooling of the ions, as discussed below, has generally been successful in removing the excess energy, at least as monitored by the chemical reaction.

2. Laser Ablation

For ion beam experiments, Anderson and co-workers[49] have developed a variation on the DLV source (which they call laser ablation) where the target is mounted on the side of a radio frequency ion trap that collects the nascent cluster ions. A pulsed jet of helium buffer gas is passed over the target just as the laser is fired. The gas pressure ($\sim 10^{-2}$ Torr) is too low to cause significant confinement of the expanding plasma plume or condensation, thus this method works only for materials which form cluster ions directly in the vaporization process. The buffer gas jet serves to begin cooling the hot nascent cluster ions, helps trap them in the radio frequency field, and sweeps them into a second radio frequency ion trap for further cooling.

3. Laser Vaporization

Perhaps the most generally applicable type of cluster ion source is modeled on the laser vaporization (LV) source originally developed by Smalley and co-workers[50] and shown schematically in Figure 6. A typical LV source consists of a 1–3-mm diameter channel, through which a pulsed or continuous flow of helium is passed. A solid rod or disk-shaped target of the cluster precursor

is mounted adjacent to the flow channel, either protruding into the flow or communicating through a small hole. Opposite the target is another small hole, through which the vaporizing laser is focused onto the target. As in the DLV source, some clusters may be generated directly in the vaporization process, but in most cases the primary function of the laser is to create a plasma of vaporized target material. The helium pressure is high enough to confine the expanding vapor plume, which is entrained in the flow. As the plug of vapor moves along the flow channel, it is cooled by the helium, and condensation into clusters occurs. At the end of the flow channel, the clusters and buffer gas undergo supersonic expansion into a vacuum chamber, and a cluster beam is formed by skimming the core of the expansion.

A major advantage of the LV technique is versatility; it appears to work well for nearly any material that can be fabricated into a solid target. The size distribution is also very impressive; different source conditions can produce intense beams of clusters containing from 2 to several hundred atoms. A disadvantage is the high helium gas load that requires an elaborate differential pumping system. For ion chemistry work, it is possible to use the ions directly produced in the LV process,[29] to inject high energy electrons into the flow,[51] or to post-ionize using either a laser[52] or electron beam.

In the LV source the gas density is high, ranging from 0.2 to several atmospheres, thus it is generally assumed that sufficient collisions occur to thermalize the clusters at the flow temperature. Spectroscopic studies have shown this to be true, at least for small clusters under appropriate source conditions;[53-55] however, there have also been a number of experiments suggesting that LV generated clusters are quite hot.[56,57] The reason for the discrepancy is not clear, but the temperature may depend strongly on source conditions in a not easily predictable fashion. For example, at Stony Brook we have experimented with two LV sources that differ only in the flow channel geometry *before* the vaporization section. For carbon cluster ions, one source generates C_x^+ in the 15-atom range that appear to be cold (from comparison of reactivity to that of clusters generated in a DLV/storage source), while under identical operating conditions, the other source produces cluster ions that react as if they contain several electronvolts of internal energy. Evidently, our "minor" change in channel geometry results in major changes in the helium flow and in the resulting cluster ions.

In any case, the assumption that LV-generated cluster ions are ipso facto thermalized appears unwarranted to us. In spectroscopic studies, hot bands provide a measure of cluster temperature and the source conditions can be adjusted to minimize internal energy. In most chemistry experiments, the cluster internal energy distribution is not measured, thus the possibility that the reactant cluster ions are hot must be considered.

4. Sputtering

Impact of high kinetic energy particles on a solid target results in sputtering of a wide variety of neutral and ionic species, including cluster ions,[58] which have been used in several chemistry studies. The projectile particles are typically either high energy atomic ions or fast atoms generated by charge neutralization of a ion beam. For ion bombardment the technique is called secondary-ion mass spectrometry (SIMS); neutral bombardment is referred to as fast-atom bombardment (FAB). SIMS is somewhat simpler; however, FAB can be used for nonconducting targets since surface charging is minimized.

Figure 5 shows the configuration used at Stony Brook.[31] The projectiles are argon or xenon atoms with kinetic energies of ~10–20 keV, impacting a metal target at an angle of 60° from the surface normal. The projectile flux is $\sim 2 \times 10^{15}$ atoms/s·cm^2, which is low enough that each impact event is isolated; thus cluster ions are produced directly in the sputtering process. While overall material removal rates may be large, the cluster ion production efficiency is low, yielding only $\sim 10^5$ size-selected cluster ions per second. Intensity can be increased significantly by using a high-current sputtering gun. For example, currents in the 1–10-nA range have been reported for Ag_x^+ ($x \leq 5$).[59] Sputtering has also been coupled to an ICR by Irion and coworkers.[60]

Sputtered cluster ions are both translationally and internally hot, as shown both by their chemical reactivity[61] and by observations of metastable decay after leaving the ion source.[62] Cooling of the nascent ions is therefore essential in chemistry studies. Sputtering appears to be able to generate cluster ions from a wide variety of metals, semimetals, and insulators. Its utility for cluster ion chemistry work is somewhat limited because the cluster size distributions generally fall off rapidly with increasing size, though Irion and coworkers[63] have reported fairly large size distributions (up to 100 atoms) for some metals.

E. Methods for Cooling Ions

Having seen that cluster ions are often produced with excess energy, what can be done to obtain ions with a near-thermal distribution of internal energy? The experimentalist has recourse to two basic schemes: either wait for radiative relaxation to occur or provide a collision partner and time for a sufficient number of collisions to remove the excess energy. Radiative relaxation rates for cluster ions are generally unknown, but it seems reasonable to treat large cluster ions as blackbody emitters. In that case, radiative energy loss scales as T^4, suggesting that initial cooling rates will be high, but that cooling all the way to room temperature will be a slow process; requiring that the cluster ions be stored for seconds before reaction. This is feasible in the FT-ICR method, but in most instruments, active cooling by collisional quenching is desirable.

In FT-ICR the typical experimental sequence can be modified to include a pulse of buffer gas with an appropriate delay for thermalizing collisions and evacuation of the buffer gas.[64] After thermalization a second set of ejection sweeps is used to remove any products formed during the cooling time. This sequence thus combined both radiative and collisional quenching.

A related technique, that has been applied by the Stony Brook group, is storage of the hot nascent cluster ions in buffer gas-filled radio frequency ion traps. This technique is an adaptation of the high-pressure, rf-storage ion source developed by Gerlich and coworkers[32] for production of thermalized molecular ions.

Technical details and applications of this technique to low-temperature ion–molecule chemistry are given in the article by Gerlich and Horning in this issue. The basic idea is that ions in a radio frequency field experience a net force directed toward regions of lower field strength. If a set of electrodes is arranged around a central volume, connected to alternate phases of a radio frequency generator, the field is strong near the electrodes and cancels in the center, thus creating an ion trap. In the Stony Brook instrument (Figure 5) the trap is in the form of a channel that follows a labyrinthine path cut into a stack of electrodes. The channel is filled with $\sim 10^{-2}$ Torr of N_2, Ar, or He buffer gas. Hot cluster ions enter at one end, lose translational energy by collisions with the buffer gas, and then diffuse through the trap and exit. Residence time is ~30 ms, which corresponds to about a thousand collisions. There is no direct way of determining how completely the cluster ions are equilibrated; however, we have examined the effects of varying the buffer gas density over several orders of magnitude. Qualitatively different chemistry is observed for low buffer gas densities, where the cluster ions are not effectively cooled, whereas for pressures above $\sim 10^{-3}$ Torr, equilibration appears to be complete, at least insofar as the chemical behavior is concerned.

F. Isomers and Annealing

For most cluster ions there will always be a number of stable isomeric structures and there is the possibility that more than one isomer may be present in cluster chemistry experiments. If the different isomers also have significantly different reactivity, this may confuse the interpretation of reaction mechanisms and cluster size effects. Multiple isomers are especially likely in materials where the barriers to isomerization are high and in experiments where the rate of cooling in the cluster ion source is fast enough to "freeze in" the higher energy isomers. Semimetals such as silicon and carbon, with their strong and directional bonding, are likely candidates. As discussed below, multiple isomers have been observed for some cluster sizes of both C_x^+ and Si_x^+. For metals, where bonding is not strongly directional, the activation barriers to interconversion between isomers are small, which should foster annealing as the nascent cluster ions cool after production.

In cases where multiple isomers are a problem, it is possible to anneal the clusters to the most stable structure. Jarrold and Honea[65] have shown that by injecting a silicon cluster ion beam into a high-pressure buffer gas at energies of 20–90 eV, the clusters are first collisionally heated, then collisionally cooled. For reaction of Si_x^+ with C_2H_4, which is strongly isomer dependent,[12] annealing is observed for injection energies above 40 eV. Another approach to annealing is laser excitation, which has been used by Maruyama et al.[66]

III. Main Group Clusters

Table I provides a summary of the literature on the chemistry of main group cluster ions during the period covered by this review. In the following sections, we will discuss some of the work on clusters of boron, aluminum, carbon, and silicon. These clusters have been the most extensively studied, allowing us to make comparisons between different clusters such as boron and aluminum, or carbon and silicon. The overlap of results from various research groups also provides useful insights into the properties and behavior of these clusters. This is particularly true for carbon and silicon, which exhibit interesting isomer behavior.

A. Boron

Boron and boron-rich solids typically have unusual crystal structures, consisting of strongly bonded networks with local icosahedral symmetry, resulting in hard refractory materials.[67] Boron hydrides and carboranes also have unusual structures; for example, $B_{12}H_{12}^-$ and $B_{10}C_2H_{12}$ are stable molecules with hollow-icosahedral structures.[68] This bonding behavior is attributed to boron's "electron deficiency", which leads to formation of multicenter bonds where three or more atoms share a single pair of electrons. How this might carry over to pure boron cluster ions is not obvious.

Hanley, Whitten, and Anderson[49] reported a combined ab initio/collision-induced dissociation study of B_x^+ (x = 2–13), in which it was concluded that the atoms form networks in which the average coordination increases with cluster size. The increasing B–B coordination is reflected in the experimental cluster stabilities, which increase rapidly with size. Starting with B_5^+, the calculated structures become three-dimensional with multicenter bonding similar to that found in boron-rich materials. Experimentally, B_{13}^+ is found to be anomalously stable, leading to the speculation that it is a filled icosahedron; a structure never seen in normal boron compounds.

More recently, Kato and co-workers[69,70] reported an ab initio molecular orbital study of B_{2-12}^+ and B_{2-12}, in which a very different structural motif was found. For most cluster sizes, they found the most stable geometry to be low symmetry planar (or pseudoplanar) rings, some of which have an atom in the middle. Bonačić-Koutecký et al.[71] have reported geometries for B_{2-8}^+ and B_{2-8} calculated at the SCF level. They find high symmetry planar or nearly planar cyclic structures, with an atom in the center for B_7^+ and B_8^+. As expected for these low-coordination geometries, the binding energy per atom increases slowly with cluster size, in contrast to the calculations and experimental observations of Hanley et al.[49] Finally, Kawai and Weare[72,73] have calculated geometries for B_{12} and B_{13} using a simulated annealing technique. They find high-coordination networks similar to, but less symmetric than, the structures proposed by Hanley, Whitten, and Anderson. They also explain the high stability of B_{13}^+ as being due to a particularly stable electronic, rather than geometric, structure.

Anderson and co-workers have used low-energy beam methods to study reactions of boron cluster ions containing up to 15 atoms, with the goal of elucidating reaction energetics and mechanisms and relating these to cluster structure. Oxidation reactions have been the most thoroughly studied, including detailed work on oxidation of B_x^+ by molecular oxygen,[74] carbon dioxide,[75] and nitrous oxide.[76] Etching of B_x^+ by water[77] and addition of hydrogen[78] have also been studied in sufficient detail to allow extraction of B_x^+–H bond

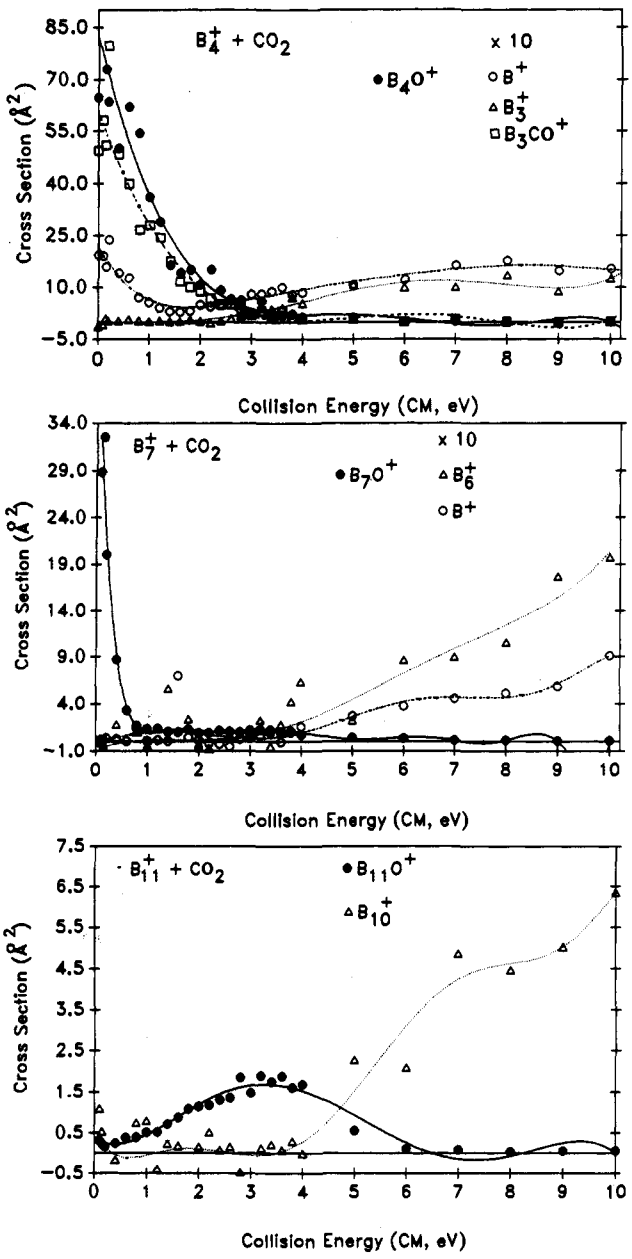

Figure 7. Absolute cross sections for reaction of several boron cluster ions with CO_2. B_4^+ shows behavior typical of small boron cluster ions, B_{11}^+ is typical of clusters in the 8–14-atom range, and B_7^+ shows transitional behavior.

energies as a function of cluster size. In addition, less comprehensive studies[79] of B_x^+ reactions with CO, CH_4, CF_4, SiH_4, N_2, C_2H_4, CH_3OH, $(CH_3)_2CO$, NH_3, HF, and CS_2 have been carried out for comparison. As an example of these studies, we will outline the results for oxidation by CO_2.

Figure 7 presents the results for reaction with CO_2 of several typical cluster ions: B_4^+, B_7^+, and B_{11}^+. For all B_x^+ ($x \leq 14$) the dominant reaction at low collision energies is formation of the oxide B_xO^+. For reactant clusters containing 2–7 and 9 atoms, oxidation proceeds with a large cross section that peaks at low collision energies, demonstrating that oxidation is exoergic with no activation barrier. At low energies, the cross sections are close to the collision cross section, indicating high reaction efficiency. For reactant clusters with 10 or more atoms, collision energy thresholds are observed, indicating that oxidation becomes endoergic or at least has an activation barrier. From comparison with thermochemical limits extracted from the data for oxidation by water, it was concluded that any activation barriers must be small and thus that oxidation is endoergic for larger boron cluster ions. B_8^+ is a transitional cluster size, showing reactivity similar to both small and large clusters. Its cross section has a small (~5 Å²) component that peaks sharply at low energies, as well as a second component that turns on at about 0.5 eV. This behavior could either indicate that B_8^+ clusters have two types of binding sites or that the cluster beam contains two isomers of B_8^+.

Assuming no barriers, and comparing thresholds observed for oxidation by CO_2,[75] O_2,[74] and water,[77] limits on the B_x^+–O atom bond energies can be estimated as a function of cluster size. $D(B_x^+\text{–O})$ is estimated to drop from ≥6.5 eV for B_2^+ to ~5.2 eV for B_{14}^+. For larger cluster ions, containing up to 24 atoms, reactivity with N_2O[76] suggests that the B_x^+–O bond energy continues to decrease with increasing size. The only significant deviation from this apparently smooth trend is B_{13}^+, with an estimated $D(B_{13}^+\text{–O})$ of ~4.4 eV. This is consistent with observations that B_{13}^+ is anomalously stable with respect to dissociation and that its low energy reactivity is typically an order of magnitude lower than neighboring cluster sizes.

The decrease in reactivity and ad-atom affinity with increasing cluster size, as observed for CO_2,[75] appears to be a general phenomenon for boron cluster ions. The CID results show that over the same range of cluster size, there is a concomitant increase in cluster stability. These trends are attributed to increasing B–B coordination for the larger cluster ions. This is expected to increase cluster stability and should also decrease reactivity due to coordinative saturation. Closer examination of the data provides further support for this picture. For small clusters such as B_4^+, where B–B coordination is low, the oxidation efficiency (i.e. $\sigma_{oxidation}/\sigma_{collision}$) is near unity at low collision energies, and decreases slowly with increasing energy. For B_7^+, reaction efficiency is lower and also decreases much more sharply with increasing collision energy. Our speculation is that for the larger reactant clusters, most sites on the cluster become coordinatively saturated. At low collision energies, the collision time is long enough to allow the CO_2 to find an unsaturated site and react. At higher collision energies, the scattering becomes direct, and reaction can only occur when the CO_2 hits a reactive site. For larger clusters, there are apparently no sites where reaction can occur at low energy, leading to threshold behavior. Weare and coworkers[80] have observed just this effect in a theoretical study of B_{12} reacting with H_2. They calculate that B_{12} has a distorted icosahedral cage structure, where one of the atoms is 3-fold coordinated and the other 11 atoms have four or more B–B bonds. Reaction is observed to occur only if the H_2 impacts the 3-fold coordinated atom.

The results on B_x^+ oxidation by O_2[74] and CO_2[75] are consistent with this picture. As might be expected given the similarity of D(O–O) and D(OC–O), oxygen reacts with the small clusters with no activation energy (though efficiency is only ~10%), while for larger B_x^+ (x = 8, 10–13) collision energy thresholds are observed. For O_2, since two O atoms are available at the cost of

Table I. Summary of Main Group Cluster Ion Chemistry Studies*

cluster	neutral†	experiment‡		refs
		apparatus	source	
CsI	SF_6	TQMS	FAB	*a*
$Mg_xO_y^+$ ($x < 8, y = x - 1, x$)	CID	TQMS	SIMS	*b*
$Ca_xO_y^+$ ($x \leq 8, y = x - 1, x$)	CID	TQMS	SIMS	*b*
B_x^+ (x = 2–16)	O_2, D_2, H_2O, CO_2	IB	DLV	74, 78, 77, 75
B_x^+ (x = 2–24)	N_2O	IB	DLV	76
B_x^+ (x = 2–13)	CID	IB	DLV	49
B_xO^+ (x = 5–9)	CID	IB	DLV	75
$B_xO_y^+$ (x = 2–9, y = 1–13)	CID	ZAB	FAB	90
Al_x^+ (x = 2–9)	O_2, N_2O	IB	FAB	87
Al_x^+ (x = 3–27)	D_2	IB	LV	*c*
Al_x^+ (x = 3–26)	O_2	IB	LV	85
Al_x^+ (x = 2–33) Al_x^- (x = 5–37)	O_2	flow tube	LV	88
Al_{25}^+	CO, N_2, O_2, CH_4, C_2H_4	IB	LV	*d*, *e*
Al_x^+ (x = 24–26)	C_2H_4	IB	LV	*f*
Al_x^+ (x = 2–6)	CID	TOF	SIMS	*g*
Al_x^+ (x = 3–26)	CID	IB	LV	33
Al_x^- (x = 3–32)	EA, O_2, CID	FT-ICR	DLV	44
$Al_xV_yNb_z^-$ (x = 2–13, y, z = 0, 1)	O_2	flow tube	LV	*h*
$Al_xO_y^+$ (x = 2–5)	N_2O, NO_2, O_2, NO, CID	FT-ICR TQMS	DLV FAB	39
$Al_xO_y^+$ (x = 2–4)	CT	FT-ICR	DLV	*i*
$Al_xO_y^+$ (x = 10–27, y = 1, 2)	D_2	IB	LV	*j*
$Al_xO_y^+$ (x = 3–26, y = 1, 2)	CID	IB	LV	86
$Al_xIn_yO_z^+$ ($x + y$ = 2, 3)	N_2O, NO_2	FT-ICR	DLV	*k*
$Al_xS_y^+$ (x = 1–7)	NO_2	FT-ICR	DLV	40
$Ga_xO_y^+$ (x = 2–5)	N_2O, NO_2, O_2, NO, CID	FT-ICR TQMS	DLV FAB	39
$Ga_xAs_y^+$ ($x + y$ = 6–16)	NH_3	FT-ICR	LV	*l*
$Ga_xAs_y^-$ ($x + y$ = 2–6)	HCl	FT-ICR	DLV	*m*
$In_xO_y^+$ (x = 2–5)	N_2O, NO_2, O_2, NO, CID	FT-ICR TQMS	DLV FAB	39
C_x^+ (x = 2–6); C_xH^+ (x = 2–5)	CO	SIFT	EI	100
C_x^+ (x = 2–12)	D_2	IB	DLV	107
C_x^+ (x = 3–20)	CH_4, C_2H_2, C_2H_4, HCN	FT-ICR	DLV	105, 46
C_x^+ (x = 6–24)	CT	FT-ICR	DLV	64
C_x^+ (x = 10–25)	aromatics	FT-ICR	DLV	*n*
C_x^+ (x = 2–15)	CID	IB	DLV	*o*
C_x^+ (x = 7, 10)	CID	ZAB	EI	106
C_x^- (x = 4–13)	F_2, C_2N_2, CID	FT-ICR	DLV	109
C_x^+ (selected $x \geq 48$)	CT	FT-ICR	DLV, EI	37, *p*
C_x^+ (x = 3–61)	mobility	ZAB/DT	LV	110
C_x^+ (x = 60, 70), C_x^- ($x \geq 60$)	PA, CH_4	FT-ICR TQMS	TD EI, CI	*q*
C_x^- (x = 60, 70)	OH acids, BF_3, NO_2, O_2, NO	FA-TQMS	EI	*r*
$C_xB_y^+$, $C_xB_y^-$ ($x \geq 44$)	NH_3	FT-ICR	LV	*s*
$C_{60}Y^+$	N_2O	FT-ICR	DLV	*t*
C_xN^+ (x = 4–8)	CH_4	FT-ICR	DLV	112, 113
$C_xSi_y^+$ (x = 1–8, y = 1, 2)	C_2H_2, unsaturated hydrocarbons, CT	FT-ICR	DLV	48, *u*, 115
$C_xTa_y^+$ (x = 1–14, y = 1, 2)	CID, D_2, CH_4, C_2H_4, C_2H_6	FT-ICR	DLV	41, 47
Si_x^+, Si_x^- (x = 2–7)	SiH_4	FT-ICR	DLV	*v*
$Si_xD_y^+$ (x = 1, 2)	SiH_4/H_2O mixture	FT-ICR	EI	*w*
Si_x^+, Si_x^- (x = 39, 43, 48)	$N(CH_3)_3$	FT-ICR	LV	*x*
Si_{3x}^+ (x = 12–17)	C_2H_4, NH_3	FT-ICR	LV	66, 117
Si_x^+ (x = 5–66); Si_x^- (x = 39–50)	NH_3	FT-ICR	LV	26
Si_x^+ (x = 10–70)	NH_3, H_2O	IB/DT	LV	*y*, 118, *z*, *aa*
Si_x^+ (x = 3–24, x = 17–48, or x = 11–50)	C_2H_4	IB/DT	LV	12, *aa*, *bb*, *kk*
Si_x^+ (x = 10–65)	O_2	IB/DT	LV	*aa*, *cc*
Si_{25}^+	D_2, CH_4, O_2, C_2H_4, CO, N_2	IB	LV	*dd*
Si_x^+ (x = 2–8), Si_x^- (x = 2–5)	CID	TOF	SIMS	*g*
Si_x^+ (x = 5–70)	CID	IB/DT	LV	*ee*, *ff*
Si_x^+ (x = 10–60)	mobility	IB/DT	LV	*gg*
Ge_x^+ (x = 39–46)	NO	FT-ICR	LV	116
Ge_x^{2+} (x = 2–11)	CT	TQMS	LMIS	*hh*
P_x^+ (x = 2–4)	CT	FT-ICR	DLV	*ii*
As_x^+ (x = 2–5)	CT	FT-ICR	DLV	*ii*
Sb_x^+ (x = 3–5)	CID	FT-ICR TQMS	DLV SIMS	*jj*
Bi_x^+ (x = 3–8)	CID	FT-ICR TQMS	DLV SIMS	*jj*
$Sb_xBi_y^+$ ($x + y \leq 4$)	CID	FT-ICR TQMS	DLV SIMS	*jj*

Table I Footnotes

* Some low-energy CID studies are also listed. † CT = charge transfer, EA = electron affinity, or PA = proton affinity studies were performed with various neutrals. ‡ Entries in this column consist of two codes for the experimental apparatus and the cluster source. Apparatus codes: DT, drift tube; FA, flowing afterglow; FT-ICR, Fourier transform ion cyclotron resonance mass spectrometer; IB, ion beam; SIFT, selected ion flow tube; TOF, time-of-flight mass spectrometer; TQMS, triple quadrupole mass spectrometer; ZAB, reverse geometry (BE) mass spectrometer. Source codes: CI, chemical ionization; DLV, direct laser vaporization; EI, electron impact; FAB, fast-atom bombardment source; LMIS, liquid–metal ion source; LV, laser vaporization; SIMS, ion sputtering source; TD, thermal desorption. [a] Callahan, J. H.; Colton, R. J.; Ross, M. M. *Int. J. Mass Spectrom. Ion Processes* **1989**, *90*, 9. [b] Saunders, W. A. *Phys. Rev. B.* **1988**, *37*, 6583. [c] Jarrold, M. F.; Bower, J. E. *J. Am. Chem. Soc.* **1988**, *110*, 70. [d] Jarrold, M. F.; Bower, J. E. *J. Am. Chem. Soc.* **1988**, *110*, 6706. [e] Jarrold, M. F.; Bower, J. E. *Z. Phys. D.* **1989**, *12*, 551. [f] Jarrold, M. F.; Bower, J. E. *Chem. Phys. Lett.* **1988**, *149*, 433. [g] Begemann, W.; Hector, R.; Liu, Y. Y.; Tiggesbäumker, J.; Meiwes-Broer, K. H.; Lutz, H. O. *Z. Phys. D.* **1989**, *12*, 229. [h] Harms, A. C.; Leuchtner, R. E.; Sigsworth, S. W.; Castleman, A. W., Jr. *J. Am. Chem. Soc.* **1990**, *112*, 5673. [i] Bach, S. B. H.; McElvany, S. W. *J. Phys. Chem.* **1991**, *95*, 9091. [j] Jarrold, M. F.; Bower, J. E. *Chem. Phys. Lett.* **1988**, *144*, 311. [k] Parent, D. C. *Chem. Phys. Lett.* **1991**, *183*, 51. [l] Wang, L.; Chibante, L. P. F.; Tittel, F. K.; Curl, R. F.; Smalley, R. E. *Chem. Phys. Lett.* **1990**, *172*, 335. [m] Reents, W. D., Jr. *J. Chem. Phys.* **1989**, *90*, 4258. [n] Zimmerman, J. A.; Creasy, W. R. *J. Chem. Phys.* **1991**, *95*, 3267. [o] Sowa, M. B.; Hintz, P. A.; Anderson, S. L. *J. Chem. Phys.* **1991**, *95*, 4719. [p] McElvany, S. W.; Ross, M. M.; Callahan, J. H. *Mat. Res. Soc. Symp. Proc.* **1991**, *206*, 697. [q] McElvany, S. W.; Callahan, J. H. *J. Phys. Chem.* **1991**, *95*, 6186. [r] Sunderlin, L. S.; Paulino, J. A.; Chow, J.; Kahr, B.; Ben-Amotz, D.; Squires, R. R. *J. Am. Chem. Soc.* **1991**, *113*, 5489. [s] Guo, T.; Jin, C.; Smalley, R. E. *J. Phys. Chem.* **1991**, *95*, 4948. [t] McElvany, S. W. *J. Phys. Chem.* **1992**, *96*, 4935. [u] Parent, D. C. In *Proceedings of the International Symposium on the Physics and Chemistry of Finite Systems: from Clusters to Crystals*; Jena, P., Khanna, K. N., Rao, B. K., Ed.; Kluwer Academic Publishers: Dordrecht, 1992; Vol. II, p 1131. [v] Mandich, M. L.; Reents, W. D., Jr.; Kolenbrander, K. D. *J. Vac. Sci. Technol. B* **1989**, *7*, 1295. [w] Mandich, M. L.; Reents, W. D., Jr. *J. Chem. Phys.* **1992**, *96*, 4233. [x] Maruyama, S.; Anderson, L. R.; Smalley, R. E. *Mat. Res. Soc. Symp. Proc.* **1991**, *206*, 63. [y] Ray, U.; Jarrold, M. F. *J. Chem. Phys.* **1990**, *93*, 5709. [z] Ray, U.; Jarrold, M. F. *J. Chem. Phys.* **1991**, *94*, 2631. [aa] Ray, U.; Jarrold, M. F.; Creegan, K. M.; Bower, J. E. *Int. J. Mass Spectrom. Ion Processes* **1990**, *100*, 625. [bb] Jarrold, M. F.; Honea, E. C. *J. Am. Chem. Soc.* **1992**, *114*, 459. [cc] Jarrold, M. F.; Ray, U.; Creegan, K. M. *J. Chem. Phys.* **1990**, *93*, 224. [dd] Jarrold, M. F.; Bower, J. E. *J. Am. Chem. Soc.* **1989**, *111*, 1979. [ee] Jarrold, M. F.; Bower, J. E. *J. Phys. Chem.* **1988**, *92*, 5702. [ff] Jarrold, M. F.; Honea, E. C. *J. Phys. Chem.* **1991**, *95*, 9181. [gg] Jarrold, M. F.; Constant, V. A. *Phys. Rev. Lett.* **1991**, *67*, 2994. [hh] Saunders, W. A. *Phys. Rev. B.* **1989**, *40*, 1400. [ii] Zimmerman, J. A.; Bach, S. B. H.; Watson, C. H.; Eyler, J. R. *J. Phys. Chem.* **1991**, *95*, 98. [jj] Ross, M. M.; McElvany, S. W. *J. Chem. Phys.* **1988**, *89*, 4821. [kk] Creegan, K. M.; Jarrold, M. F. *J. Am. Chem. Soc.* **1990**, *112*, 3768.

breaking one bond, about 5 eV more energy is available in the activated complex than for CO_2. This evidently doesn't affect the activation energies, but it has a major effect on product ion distributions. Rather than simply forming B_xO^+, fragmentation occurs, producing a variety of daughter ions.

For N_2O, the weak (1.67 eV) N_2–O bond allows boron cluster ions containing up to 18 atoms to react with no activation barrier. Since only one O atom is available, the dominant oxidation product is B_xO^+. Another interesting result is that reactant ions containing 2–6, 9, and >15 atoms form significant amounts of B_xN^+ products, even though the N–NO bond is three times stronger than the N_2–O bond. It was speculated that nitride products were indicative of reactant clusters containing binding sites allowing a nitrogen atom to bond to 3 boron atoms. Formation of the additional B–N bond might drive N–NO bond scission.

B. Aluminum

Aluminum has physical and chemical properties that are quite different from boron, despite the fact that the two elements are isovalent.[81] These differences are also found in Al_x^+ and B_x^+. For example, both CID[31,33] and photodissociation[82] indicate that the stabilities of Al_x^+ ($x \leq 17$) are less than 3.3 eV, which compares with values up to 8 eV for B_x^+ in the same size range. Both B_x^+ and Al_x^+ exhibit oscillations in stability with cluster size; however, electronic shell closing effects seem to be much more important in aluminum clusters. Another similarity is that both B_x^+ and Al_x^+ decompose primarily by evaporation of single atoms, and the stabilities of both increase with size. This has been interpreted to suggest that Al_x^+ have compact 3-dimensional structures, which is consistent with ab initio calculations of aluminum cluster structures by Upton[83] and by Pettersson and co-workers.[84]

The chemistry of Al_x^+ has been studied using beam techniques by Anderson and co-workers and by Jarrold and co-workers. More recently Castleman and co-workers have used flow-tube techniques to study the chemistry of both Al_x^+ and Al_x^-. Table I lists the reactions studied with references; for brevity this section will focus on the oxidation chemistry.

Jarrold and Bower[85] used low-energy beam techniques to measure cross sections and branching ratios for reaction of Al_{3-26}^+ with O_2 at collision energies of 1.2 and 4.2 eV. Clusters containing more than 12 atoms had a propensity to lose four aluminum atoms, conjectured to be due to the following reaction:

$$Al_x^+ + O_2 \rightarrow Al_{x-4}^+ + 2Al_2O$$

Smaller clusters lost five atoms, presumably as either $Al_2O + Al_3O$ or $2Al_2O + Al$. Smaller clusters also gave a variety of products. The Al_2O loss mechanism is supported by measurements of CID branching ratios for fragmentation of $Al_xO_y^+$ ($y = 1,2$).[86] After collisional activation, the $Al_xO_y^+$ loses Al_2O molecules.

Ruatta and Anderson[87] studied $Al_{1-9}^+ + O_2$ in greater detail, measuring cross sections over the collision energy range from 0.25 to 10 eV. They also looked at oxidation by N_2O to obtain further insight into the oxidation mechanism and energetics. Figure 8 shows typical data for the reaction with O_2. Product branching ratios and cross section magnitudes are in good agreement with Jarrold and Bower, but some additional details are clear. Note that the small Al_x^+ ions react with no activation barrier, while for $x > 6$ barriers are observed. In all cases, substantial fragmentation is observed, suggesting that oxidation is quite exoergic. Thermochemical values are difficult to estimate for large reactant clusters, however for Al_4^+ one can put reasonable limits on the energetics of the main reaction channels:

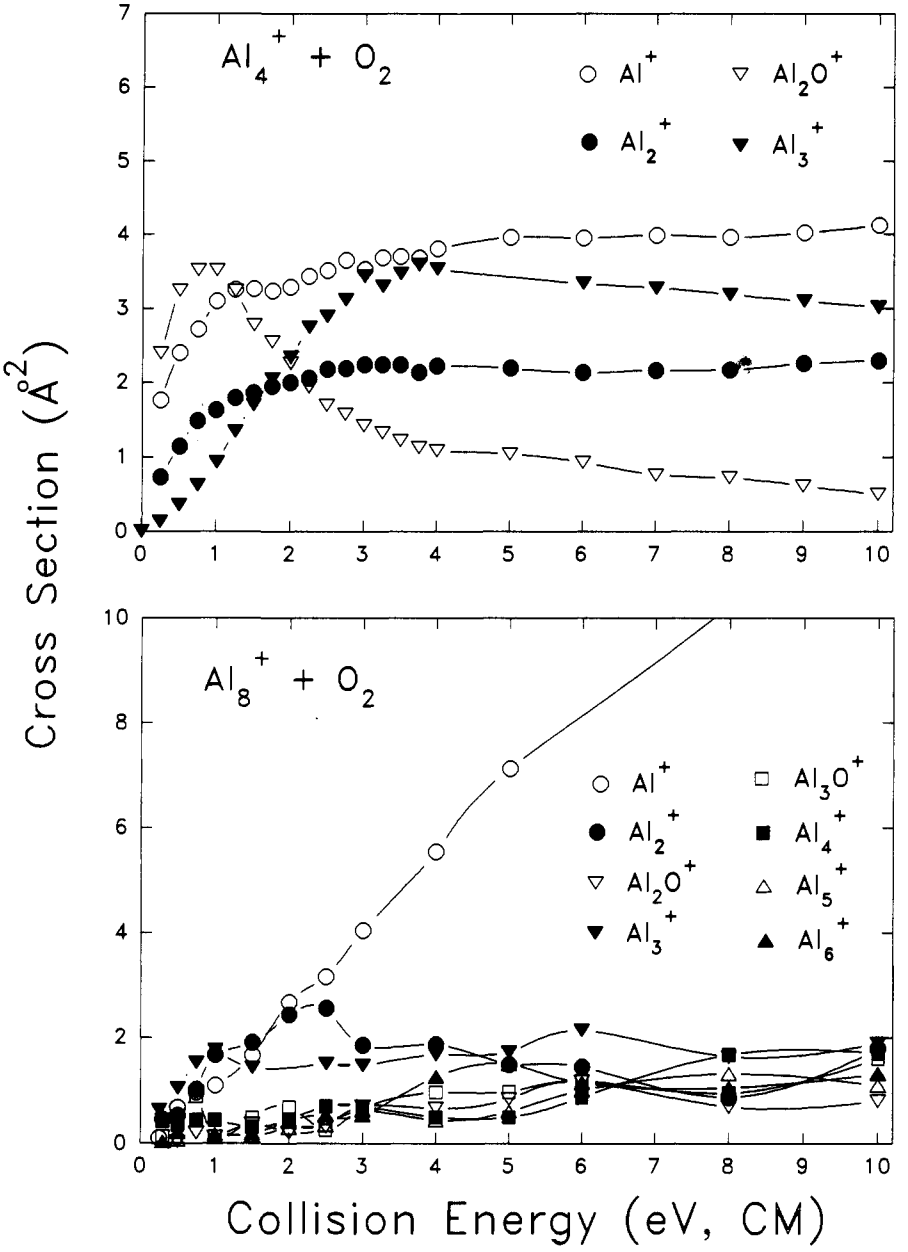

Figure 8. Absolute cross section for reaction of typical small aluminum cluster ions with O_2. Note extensive fragmentation in the products, due to the large reaction exoergicity relative to the binding energy of Al_x^+.

$Al_4^+ + O_2$

$\rightarrow Al_2O^+ (+ Al_2O)$	$\Delta H \approx -10$ eV
$\rightarrow Al^+ (+ AlO + Al_2O)$	$\Delta H \approx -7$ eV
$\rightarrow Al_2^+ (+2 AlO)$ or $(+ Al_2O + O)$	$\Delta H \approx -2.5$ eV
$\rightarrow Al_3^+ + AlO_2$	$\Delta H \approx -3$ eV

Both Jarrold and Bower and Ruatta and Anderson concluded that the oxidation mechanism involved dissociative addition of oxygen to the cluster, followed by fragmentation of the activated complex:

$$Al_x^+ + O_2 \rightarrow [Al_xO_2^+]^\dagger \rightarrow \text{products}$$

Ruatta and Anderson proposed that the observed activation barriers occur early in the reaction, arising from the need to break the O_2 (or N_2O) bond.

Leuchtner et al.[68] used a non-mass-selected flow-tube instrument to examine reaction of Al_{1-33}^+ and Al_{5-37}^- with O_2. Since they do not mass select the reactant cluster ions and the beam experiments have shown the major product to be smaller aluminum clusters (at least for the cations), their ability to study the detailed chemistry is limited. Under multiple collision conditions, they can measure the net rate of intensity change for the various size reactants. For the cations, the rates are nearly size independent at $\sim 10^{-12}$ cm^3/s, except for Al^+ and Al_7^+ which are "unreactive" for two reasons. The reaction of Al^+ with O_2 is endoergic, and the beam experiments of Ruatta and Anderson showed that $Al_7^+ + O_2$ has a high activation barrier; neither should react under thermal conditions. In addition, Al^+ and Al_7^+ are favored products from oxidative fragmentation of higher Al_x^+, and this interferes with measuring disappearance rates.

For the anions, Hettich[44] has used FT-ICR methods to examine reactions with a number of molecules. With O_2, Al_{3-6}^- react to produce AlO^- and AlO_2^-. For Al_{8-32}^- the same ionic products are observed; however, the

reactivity of even-size cluster anions is generally higher than for odd-size reactants. Quantitative rates were not reported. Leuchtner et al.[88] measured rate constants for non-mass-selected Al_{5-37}^- reacting with O_2. They report rate constants of $\sim 10^{-12}$ cm^3/s for most cluster sizes and observed that even size clusters are a factor of 2–5 more reactive than odd, in agreement with Hettich. Al_{13}^- and Al_{23}^- were unreactive.

King et al.[39] have characterized the cluster ions produced by FAB or DLV of the group 13 metal (Al, Ga, and In) oxides. The small aluminum oxide cations dissociate by loss of AlO, O or O_2, in contrast to the larger aluminum oxide ions which lose Al_2O, as discussed above. The reactions of the small aluminum oxide cations $Al_xO_y^+$ (x = 2,3 and y = 1–5) with four different oxidizing gases were also investigated with FT-ICR. Starting from the most abundant oxide cations in the FAB or DLV spectra, e.g. Al_2O^+ and $Al_3O_2^+$, oxidation with N_2O or NO_2 leads to the final species $Al_2O_4^+$ and $Al_3O_4^+$ (with N_2O) or $Al_3O_6^+$ (with NO_2) respectively. (With O_2 and NO the first addition of oxygen was either slow or did not take place in the FT-ICR.) Although these final species have high formal aluminum oxidation states, the formation of the fully coordinated structures shown

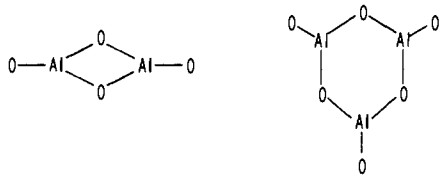

appears to be driving the oxidation. These structures were obtained from MNDO calculations as being the most stable. The $Al_2O_4^+$ structure has been proposed by Drowart et al.[89] while the $Al_3O_6^+$ structure is analogous to one proposed by Doyle[90] for sputtered boron oxide cations.

C. Carbon

1. Pure Carbon Clusters

Small carbon cluster ions are probably the best system for exploring the interrelationship between cluster structure and chemistry. Structural information can be used to refine reaction mechanisms, and at the same time, patterns of chemistry can be used to elucidate structure. The many theoretical studies on the structures of neutral and positively charged carbon clusters containing less than 10 atoms have given conflicting results.[91-98] Linear configurations with multiple bonds are generally favored for small clusters; however, some studies have predicted that clusters with 4, 6, and 8 atoms are most stable in the cyclic form. One would expect that the cyclic form would become most stable as cluster size increases, due to the reduction in strain energy. The difference in energy between cyclic and linear forms is often calculated to be quite small, however. The proposed structures for the linear clusters have reactive carbene sites (a pair of nonbonding electrons) at the ends of the chain, as shown:

$$[:C—C_{x-2}—C:]$$

Recent spectroscopic investigations of the neutral carbon clusters have mainly observed linear structures, particularly for gas-phase clusters formed by laser vaporization.[99]

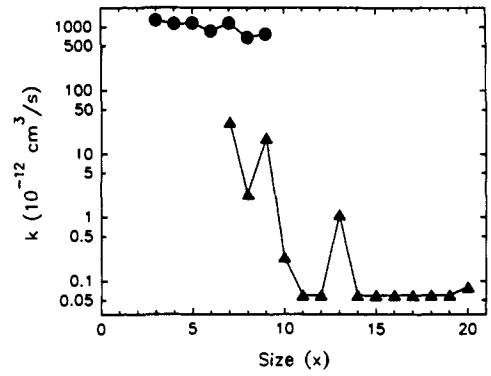

Figure 9. Rate constants k for the primary reaction of C_x^+ with HCN, plotted vs cluster size for the "linear" (●) and "cyclic" (▲) forms. The values for x = 11, 12, and 14–20 are upper limits as no reaction was observed. The plot shows the existence of two isomers for x = 7–9 and the large drop in reactivity between x = 9 and 10. (Data taken from ref 46.)

Bohme and co-workers[100-103] have studied the reactions of many carbon-based ions and showed that their chemistry is consistent with what is known about the chemistry of neutral carbenes. In addition, the number of carbene sites in a molecule per ion can be deduced by observing the number of sequential reactions that the species undergoes. Reactions at the carbene site are typically rapid and involve bond insertion followed by fragmentation of the transition state. These carbene sites are absent in the cyclic structures, and this lack should manifest itself through differences in the reactivity of the larger, cyclic clusters. Evidence for this change in structure was obtained in FT-ICR experiments performed by McElvany and co-workers[104,105] on the reactions of C_x^+ (x = 3–20) with a variety of small neutrals. A dramatic decrease in reaction rate constant from C_9^+ to C_{10}^+ was observed, consistent with a change from a linear, reactive carbene form to a cyclic, nonreactive form.

These experiments also revealed that C_7^+ reacts at two different rates. Such behavior can be caused by excess internal energy in the ions. However, both collisional cooling of the ions (see section II.E) and excitation of the ion kinetic energy had no effect on the observed kinetic behavior, suggesting that it is not due to excess internal or kinetic energy.[104] Instead, it was postulated that C_7^+ exists as both linear and cyclic isomers with the concomitant differences in reactivity. Later work by Parent and McElvany[46] on C_x^+ reactions with HCN showed that C_8^+ and C_9^+ also are present as two isomers, analogous to C_7^+. Figure 9 graphically presents the differences in reactivity between linear and cyclic configurations, and shows the presence of isomers for the x = 7–9 clusters.

The production method appears to have no effect on the formation and relative population of the two isomers of C_7^+. Whether produced by laser vaporization of graphite or diamond, or by CID of C_{10}^+, approximately one-third of the C_7^+ formed were reactive.[104] This is an intriguing result, especially since the cyclic isomer is calculated to be more than 2 eV higher in energy than the linear isomer. In some related work, the high-energy CID spectra of C_7^+ and C_{10}^+ ions produced by electron

impact on two $C_{10}Cl_8$ isomers (bicyclic and fused bicyclic structures) were found to be independent of the source molecule.[106] The authors could not conclusively assign structures to the ions they formed, yet the predominance of the C_3 loss suggests that the ions have the same structures as those formed by laser vaporization.

Hintz et al.[107] investigated the $C_x^+ + D_2$ system to examine how the cyclic and linear isomers react over a wide range of collision energies. Reactant cluster ions were produced in a source similar to the DLV source used in the FT-ICR work described above. As expected, the reaction cross sections for small clusters peak at low collision energies, while for C_8^+ and $C_{x\geq10}^+$, thresholds of up to several electronvolts are observed. For the intermediate sizes, where both linear and cyclic reactants are present, both low- and high-energy components appear in the cross sections. The beam results at a collision energy of 0.1 eV agree well with both the reactivity and product branching measured in the FT-ICR.

Though the carbon cluster cations containing 10 or more atoms are usually nonreactive, there are some exceptions. The x = 10–14 ions form association products with acetylene, albeit at a reduced rate. With ethylene, observation of fragmentation products from x = 10–13 provides evidence for ring-opening and subsequent carbene site reaction.[105] The energy for ring opening comes from the initial complexation step, thus ring opening is very dependent on the neutral reagent.

Beam experiments have also been completed for the reaction of C_x^+ with O_2.[108] As was observed with other neutrals, the small linear C_x^+ react with no activation energy, yielding $C_xO^+ + O$ at low energies and $C_{x-1}^+ + O + CO$ at high energies. For the cyclic clusters, two reaction mechanisms appear to be operative. Oxygen can add directly to one of the C–C bonds in a concerted process with an activation energy of a few tenths of an electronvolt. This appears to open the ring to produce a linear O–$(C)_x$–O intermediate which undergoes CO elimination to yield $C_{x-2}^+ + 2CO$. Less frequently CO_2 (or CO + O) elimination can occur. At collision energies around 3–5 eV, a second mechanism turns on, producing a variety of fragment ions. This was attributed to a sequential ring opening/oxidation mechanism.

There have been very few reactivity studies of carbon cluster anions. The small clusters are generally unreactive, due to the high electron affinities of the neutral clusters, although they do react with highly electronegative neutral reagents such as F_2 and C_2N_2.[109] In this study all ions containing 5–13 atoms were reactive, indicative of linear configurations. There was no evidence for isomeric forms of the anions, in contrast to what is seen for the cations. The results of the reaction with cyanogen are particularly interesting in demonstrating how differences in bonding can affect the chemistry. The bonding in linear carbon chains can be either cumulene-like or polyacetylene-like. While both odd and even number clusters can have cumulene-like bonding (shown on the left), only even number clusters can exhibit polyacetylene-like bonding (shown on the right):

$$[:C{=}C{=}C{=}C{=}C:] \qquad [\cdot C{\equiv}C{-}C{\equiv}C{-}C{\equiv}C\cdot]$$
(cumulene) (polyacetylene)

In the reaction with C_2N_2, the even x anions add CN and also C_2N_2 while the odd x anions only add C_2N_2. The CN addition products and the association products $C_xC_2N_2^-$ from odd x anions react further with cyanogen by adding a second molecule of C_2N_2, whereas the association products from even x anions do not react further. One possible explanation for this latter observation is that the first cyanogen is dissociated to two CN fragments which are bound to both ends of the ion, as shown:

$$[NC{-}C{\equiv}C{-}C{\equiv}C{-}C{\equiv}C{-}CN]^-$$

The CID fragmentation patterns of the various reaction products support a polyacetylene structure for the even number anions; the C_xCN^- (even x) lose C_2 instead of C_3 as is usually observed for carbon clusters. The $C_xC_2N_2^-$ product ions lose C_2N_2 when x is odd but they lose CN when x is even, in agreement with the structure above.

The C_5^- association product ion is unusual in that it is produced in both reactive and unreactive forms. These two forms behave analogously to the odd and even x association products described above. The unreactive ion may result from isomerization of the initial branched adduct, which is reactive, to a linear form that is similar to the unreactive even x product ions, as indicated:

$$\underset{\text{(reactive)}}{[:C{=}C_3{=}C(CN)_2]^-} \rightarrow \underset{\text{(unreactive)}}{[NC{-}C{=}C_3{=}C{-}CN]^-}$$

One application of ion–molecule reactions is charge-transfer bracketing using neutral reagents of known ionization potentials (IP) to determine the IPs of other species. In this technique, an ion I^+ is reacted with the neutral N and the occurrence/nonoccurrence of charge transfer is noted. If charge transfer is observed, then the IP of neutral I is greater than that of N, and vice versa. Reaction with a series of neutrals of different IP can bracket the IP of I, limited only by the availability of suitable neutral reagents. This method has been applied to a variety of clusters, including carbon. The major point of concern in obtaining accurate ionization potentials by this method is that the ions must not contain excess energy which could lead to inflated IP values. A burst of buffer gas along with a thermalization period is used in these experiments to cool the ions.[64,37] Results for pure carbon clusters containing 6–24 atoms show that those with $4x + 3$ atoms have IPs that are low compared to adjacent clusters.[64] This suggests that the larger $4x + 3$ cations (with $4x + 2$ π-electrons) are aromatic. Interestingly, there was no clear break in IP vs cluster size which would indicate a change from linear to cyclic structures.

To finish this section on pure carbon clusters we will discuss the very recent drift cell mobility measurements of Bowers and co-workers.[110] The mobility of an ion through a neutral gas (typically He) under the influence of a weak electric field is governed by the interaction potential and thus is dependent on the "shape" of the ion. In these measurements, arrival time distributions of the mass-selected ion consisted of one or more peaks corresponding to different mobilities. A plot of the mobility vs cluster size for carbon cluster cations having 3–60 atoms (Figure 10) reveals several curves, corresponding to families of clusters. This technique does not give any details about the structures themselves, but it does provide a very nice way of observing and

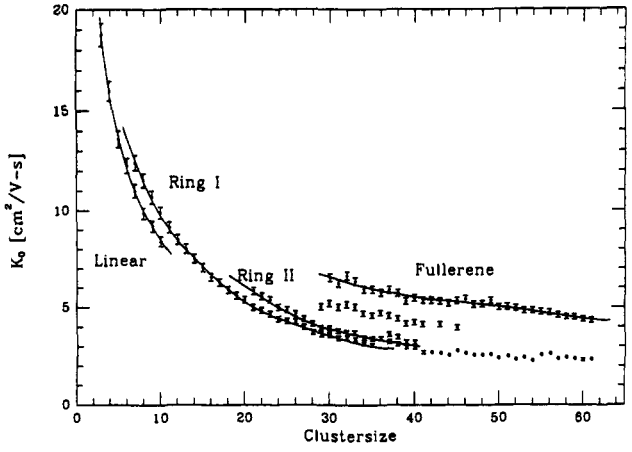

Figure 10. A plot of the mobilities measured for size-selected carbon cluster cations C_x^+. Clusters containing 7–10 and 21–61 atoms exhibit at least 2 different mobilities, which are interpreted as corresponding to different isomers. Guidelines are drawn through the four labeled families of isomers. (Ring I and ring II are postulated to be planar monocyclic and bicyclic structures respectively.) (Adapted and reprinted from ref 110. Copyright 1991 American Institute of Physics.)

categorizing changes in structure with size. Of particular interest here are the two curves labeled "linear" (for $x = 3$–10) and "ring I" (for $x \geq 7$). This is in excellent agreement with the reactivity results discussed above.

2. Substituted Carbon Clusters

A variety of substituted carbon cluster cations, including hydrogenated carbon clusters, have been studied, particularly at the Naval Research Laboratory and at York University. In this review the focus will be on clusters with elements other than hydrogen. Bohme[111] has recently reviewed the hydrogenation of carbon cluster cations and discussed the implications for interstellar chemistry.

Substituted carbon clusters can be formed as the products of ion–molecule reactions of pure carbon cluster ions, or they can be produced directly by the same techniques used to make other clusters. The geometry of clusters which are the products of ion–molecule reactions is constrained to some extent by the geometry of the reactant cluster, whereas the structure of directly produced clusters reflects the cluster growth conditions. In the rest of this section we will discuss carbon clusters containing nitrogen, silicon, and tantalum. The nitrogen-substituted clusters are formed by the reaction of carbon cluster cations with HCN, while the silicon- and tantalum-substituted clusters are produced by direct laser vaporization of solid samples made of graphite and powdered silicon or tantalum. Emphasis will be on the reactions of the monosubstituted clusters, C_xX^+, and comparison to the pure carbon clusters. The results to be discussed are presented in Figure 11.

Parent[112,113] has studied the reactions of C_xN^+ with methane and discussed the formation of cyanopolyacetylenes and the implications for interstellar chemistry. This study shows the remarkable versatility of FT-ICR in studying sequential reactions, even with different reagent gases. The reaction sequence is given in eqs 2–4:

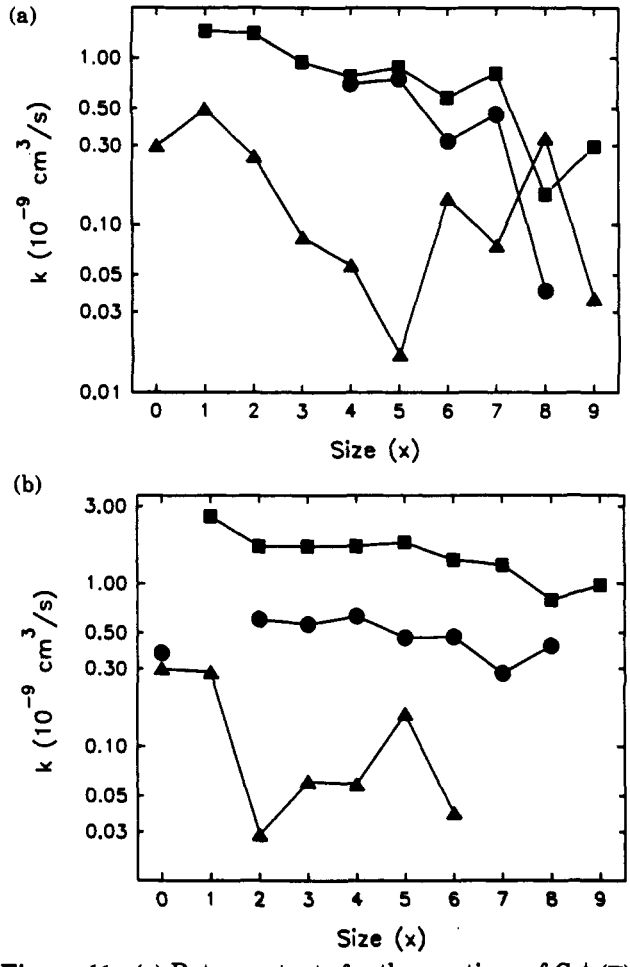

Figure 11. (a) Rate constants for the reactions of C_x^+ (■), C_xN^+ (●), and TaC_x^+ (▲) with CH_4 plotted as a function of the number of carbon atoms in the cluster. (Data taken from ref 105 for C_x^+ ($x = 3$–9), ref 112 for C_xN^+, and ref 47 for TaC_x^+. For C^+ and C_2^+ average values from the literature were used.) (b) Rate constants for the reactions of C_x^+ (■), SiC_x^+ (●) and $Si_2C_x^+$ (▲) with C_2H_2 plotted as a function of the number of carbon atoms in the cluster. (Data taken from ref 105 for C_x^+ ($x = 3$–9) and ref 48 for SiC_x^+ and $Si_2C_x^+$. For C^+ and C_2^+ average values from the literature were used.)

$$C_{graphite} + h\nu \rightarrow C_x^+ \quad (2)$$

$$C_{x-1}^+ + HCN \rightarrow C_xN^+ + \text{other products} \quad (3)$$

$$C_xN^+ + CH_4 \rightarrow \text{products} \quad (4)$$

(The reactant ions in eqs 3 and 4 are mass selected.) Some of the C_xN^+ ions formed by reaction 3 were internally excited. For these ions, $x = 4$, 6, and 8, the subsequent association reaction with HCN was sensitive to this excess energy. However, experiments performed with and without a relaxation sequence gave the same results for the reaction with methane (eq 4), indicating that this reaction is relatively insensitive to the energy content of the ions.[112]

The results can be compared with the previous work[105] on bare carbon clusters reacting with methane (Figure 11a). The variation in rate constant k is the same for C_x^+ and C_xN^+, odd x ions are more reactive than neighboring even x ions, with a substantial decrease in k at $x = 8$ being observed. The ratio of rate constants $k(C_xN^+)/k(C_x^+)$ is not constant but decreases from about 1 to 0.5 with increasing size. This was attributed to the

lower probability (as the size increases) of orienting the carbene end of the C_xN^+ toward the neutral reagent.[113] As discussed below, reaction occurs at the carbon end of the ion and not at the nitrogen end.

Similar types of products are formed in both reactions, although the presence of the nitrogen does increase the variety of products observed in the C_xN^+ reaction, due to the formation of stable cyanoacetylene species. The use of ^{13}C-labeled methane as the reagent demonstrated that rearrangement of the carbon skeleton does occur to a moderate extent.[113] The prevalence of rearrangement observed in the reaction of odd x and even x reactant ions is quite different; it is very minor for $x = 5$ and 7 but a significant fraction for $x = 4$, 6, and 8. MNDO calculations on the structures and ΔH_f of the reactants and products suggest that differences in the overall energetics are most responsible for the variations in reactivity between odd and even x ions. The MNDO calculations also show that N attack is energetically less favorable than C attack, and the observed products are most consistent with carbene attack.

More recently, Parent[48] has also investigated the reactivity of silicon carbide cluster cations, containing one or two silicon atoms, with acetylene. The variation in rate constant with size for SiC_x^+ is the same as that for C_{x+1}^+ (see Figure 11b), in contrast to the results for C_xN^+ discussed above. In addition, both ions yield the same products, suggesting that one silicon atom substitutes in for a carbon without significantly perturbing the electronic and geometric structure. This is not too surprising, since carbon and silicon are isoelectronic. However it does imply that the Si is at the end of the carbon chain, since it does not readily form multiple bonds, which would be required if it were inserted in the chain. Reaction may be occurring at both the carbon and silicon ends, since the ratio of rate constants $k(SiC_x^+)/k(C_{x+1}^+)$ does not vary with size, in contrast to the behavior of C_xN^+. Since small silicon[114] and carbon cluster cations both react with acetylene to form the same products, one cannot differentiate the reactive site through these comparisons.

The disilicon carbide ions, $Si_2C_x^+$, with $x \geq 2$ show interesting reactive behavior. The reactions of ^{13}C-labeled ions with various unsaturated reagents provides evidence for cleavage of carbon–carbon multiple bonds. The most striking example is with acetylene, where the labeling experiment reveals catalytic cleavage of the triple bond through carbon scrambling:

$$Si_2{}^{13}C_x{}^+ + {}^{12}C_2H_2 \rightarrow Si_2{}^{13}C^{12}C_{x-1}{}^+ + {}^{13}C^{12}CH_2$$

(The neutral product is assumed to be C_2H_2 since the lowest fragmentation pathway to form $C_2H + H$ would require 133 kcal/mol.) This bond cleavage is not observed for the monosilicon carbide ions in analogous experiments. There are several possible explanations for why this may be: the carbon-exchange reaction may not be kinetically competitive in the reactions of the SiC_x^+ ions; strong carbon–carbon bonding in the linear SiC_x^+ may make it energetically unfavorable; or the mechanism of the bond cleavage may involve an active site with two silicon atoms.

The $Si_2C_x^+$ also exhibit unusual nonlinear kinetics. The delayed onset of the normal linear kinetics may be attributed either to excess energy in the ions or to isomerization of the ion to a more reactive form. These two effects are difficult to differentiate, as collisions are the means of removing excess energy or effectuating the isomerization. The most definitive experiment involved the charge transfer reaction of $Si_2C_2^+$ with fluorobenzene (IP = 9.20 eV). The initial ion population charge transfers while the reactant ions present at longer reaction times do not. Isolating these ions at longer times and exciting their kinetic motion does not induce charge transfer, thus strongly implying that kinetic excitation of the initial ion population is not responsible for their observed behavior.[115]

Cassady and McElvany[47] have looked at the reactions of TaC_x^+ with D_2 and several small hydrocarbons. We will discuss the reaction with methane for comparison with the results presented above. The reactions of the tantalum carbide ions proceed at a much slower rate when compared to the pure carbon cluster ions, as seen in Figure 11a. In addition the variation of k with cluster size is clearly different than that observed with C_x^+ or C_xN^+. The most obvious example of this is for TaC_8^+, which is the most reactive ion in the series, whereas previous studies find a significant drop in reactivity when the cluster increases from seven to eight carbons. The tantalum carbide ions yield only two products, corresponding to H_2 or C_2H_2 loss from the adduct. In contrast the bare carbon cluster cations and the nitrogen-substituted clusters form a variety of products, including these two channels. Taken together, these results suggest that tantalum plays an active role in the reactions. Further evidence along these lines comes from the ^{13}C-labeling results where almost complete carbon scrambling is observed in the acetylene elimination channel. This observation strongly supports the metallocene or metallacycle structures for the TaC_x^+ ions shown:

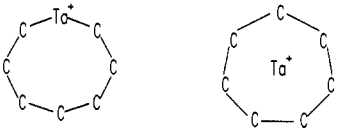

These structures lack a carbene site, which helps explain the differences in reactivity.

Evidence for isomers was seen in the reactions of TaC_x^+ ($x = 7$–9 and 11), reminiscent of observations on pure carbon cluster cations. The reaction of TaC_7^+ with D_2 is particularly interesting in this respect. The decay curve has a humped appearance (see Figure 12), similar to what was seen in the reaction of C_7^+ with HCN.[46] One possible explanation is that collision-induced isomerization from a nonreactive to reactive form is occurring. This may not be an uncommon phenomena as it also appears to occur in the reactions of $Si_2C_x^+$ examined above, and perhaps also in niobium cluster reactions.[17] Another possibility is that multiple collisions are necessary before the adduct product can be observed. Note that appearance of the $TaC_7D_2^+$ product corresponds to the onset of the more rapid decay of TaC_7^+.

D. Silicon

The reactions of small silicon cluster cations have been extensively studied by Mandich, Reents, and their co-workers utilizing FT-ICR techniques. Most of this work has been previously reviewed in detail.[3,4]

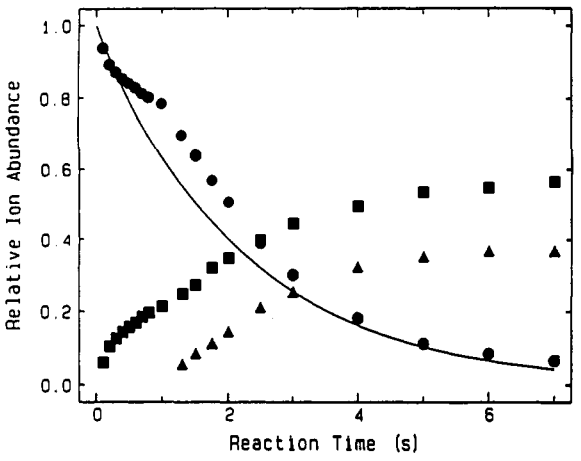

Figure 12. Reactant and product ion intensities for TaC_7^+ (●) reacting with D_2 to form TaC_5^+ (■) and $TaC_7D_2^+$ (▲). The D_2 pressure is 2.0×10^{-7} Torr and xenon buffer gas has been added to give a total pressure of 1.3×10^{-6} Torr. The decay of TaC_7^+ deviates strongly from the biexponential fit line. (Adapted and reprinted from ref 47. Copyright 1990 American Chemical Society.)

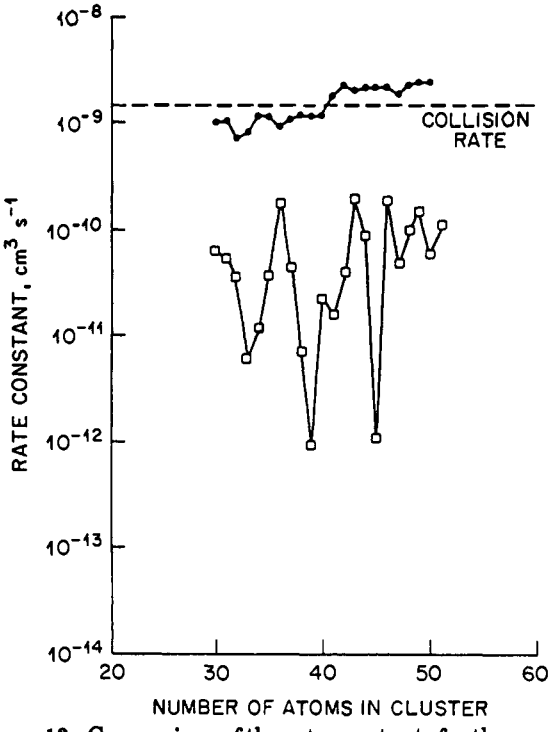

Figure 13. Comparison of the rate constants for the reaction of Si_x^+ with NH_3, measured using the ion drift tube technique (●) and FT-ICR (□) at room temperature. (Adapted and reprinted from ref 118. The FT-ICR data are from ref 26. Copyright 1991 American Institute of Physics.)

In this review we will focus on the larger ($x > 10$) silicon cluster cations, which provide a vivid example of how different cluster ion formation/reaction techniques can lead to radically different results. Jarrold and co-workers at Bell Labs and Smalley and co-workers at Rice University have published extensively on the reactivity of silicon cluster ions. The differing experimental approaches of the two groups are in some way responsible for the conflicting results they have obtained, one example of which is shown in Figure 13. For this reason we will describe in some detail the instrumentation and techniques used by each group, as well as the experimental results.

Smalley and co-workers form cluster ions by pulsed laser vaporization of a solid sample. (See the discussion of the laser vaporization source in section II.D.3 for more details.) In the most recent version of their apparatus, the cluster ion beam is directly injected into an FT-ICR cell where the ions are trapped.[116] Immediately after injection the ions may have up to 10 eV of translational energy. In addition, the ions may have internal energies well above 300 K. The ions are allowed to undergo hundreds to thousands of collisions with argon to thermalize them to room temperature, then a reactant gas is introduced into the cell.[117] The SWIFT technique is used to mass select the ions of interest. (As noted in section II.B, there is less excitation of nearby mass ions with this method of ion selection.) In some of their work, an ArF excimer laser was used to reionize clusters with more than 25 atoms.[26] As was later shown, this may have provided some measure of annealing of the clusters, as discussed in more detail below.

Jarrold and co-workers' experiment is quite different. They use a low-pressure continuous-flow LV source for Si_x^+, mass select the ions, and then inject them into a high-pressure drift cell. In the cell, the cluster ions are "drifted" through a buffer gas by an applied voltage gradient, thus establishing quasi-thermal conditions, where the clusters undergo many collisions with a well-defined average energy. Adding a reactant to the buffer gas allows reactions to occur, and varying the cell temperature allows reaction rate vs temperature measurements. At the end of the cell, the ion distribution is sampled and mass analyzed. By injecting at low energies, the Si_x^+ reactant clusters are representative of the nascent clusters from the source. Jarrold and Honea[65] have shown that injection at energies above 40 eV results in collisional annealing of the reactant cluster ions. Their technique is sufficiently refined to allow measurements of absolute reaction rates over a wide temperature range.

In reactions with ethylene and ammonia, the Rice group finds that certain size clusters are much less reactive than others. These "special" clusters are x = 21, 25, 33, 39, and 45. With ethylene, x = 48 is also less reactive than the most reactive clusters. This result is reproducible and apparently independent of the argon thermalization period. Smalley has proposed a filled fullerene structure for these "special" clusters.[26] They have also observed variations in reactivity as a function of the number of reactive collisions, indicative of the presence of isomers for some cluster ions.[26,117] Irradiation of the thermalized cluster ions with a XeCl excimer laser, followed by a second thermalization period, induces changes in the reactivity, as seen in Figure 14. The authors observed that the "special" clusters with 39, 45, and 48 atoms become even less reactive while the clusters with 36, 42, and 51 atoms become more reactive. This is interpreted as an annealing process in which one form of the ion is converted into another form.

Figure 13, which compares the results of the Bell Labs and Rice University groups for the reaction of size selected silicon cluster cations with ammonia, deserves some comment. The Rice University measurements are on photoionized clusters, thus they may have been inadvertently annealed. This is supported by the lack of evidence for isomers in this size regime,

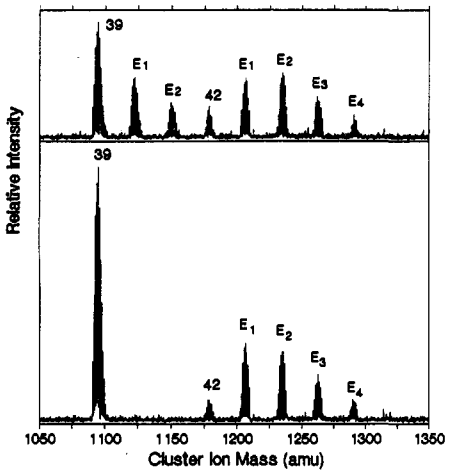

Figure 14. FT-ICR study of ethylene chemisorption on selected silicon clusters formed in an external source and injected into the ICR cell. In the top panel Si_{39}^+ and Si_{42}^+ have undergone 5000 collisions with C_2H_4. In the bottom panel the same reaction study is performed after annealing the cluster ions with 30 pulses of a XeCl excimer laser at 1 mJ/cm^2. The annealed Si_{39}^+ now displays no evidence of any reactivity while the annealed Si_{42}^+ remains highly reactive. (Adapted and reprinted from ref 66. Copyright 1990 American Institute of Physics.)

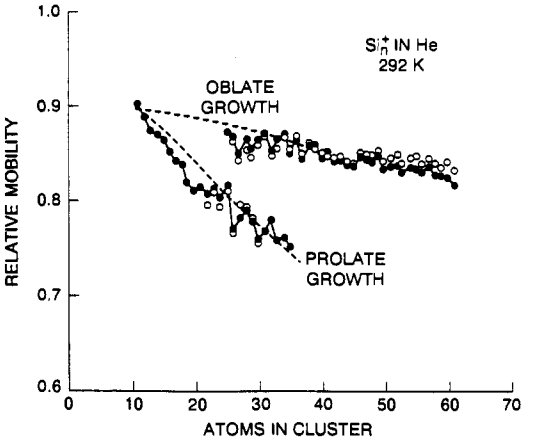

Figure 15. Mobilities of silicon cluster ions (relative to hard sphere mobilities) as measured by Jarrold and Bower. Small Si_x^+ appear to have structures which are prolate or sausage shaped, and large clusters adopt a more spherical or oblate form. For 24–34 atom clusters, both types of isomers are observed. (Reprinted from ref 119. Copyright 1992 American Institute of Physics.)

while many smaller clusters, for which no photoionization laser was used, and larger clusters, which were perhaps incompletely annealed, give evidence of 2 or more isomeric forms. Secondly, the absolute rate constants for the FT-ICR results may be off by as much as a factor of 10, due to inadequate calibration of the ammonia pressure. Nonetheless, it is clear that Smalley and co-workers observe a vastly different size dependence in these reactions than Jarrold and co-workers.

Jarrold et al.[118] have reported an elegant set of experiments that help clarify what is going on in their experiments. They have examined the *absolute* reaction rates and saturation "coverages" for Si_x^+ in ammonia as a function of temperature. The results indicate that at room temperature the dominant process is molecular chemisorption, with Si_x^+–NH_3 binding energies around 1 eV. The rates in this regime are near the collision rate, and little cluster size dependence is observed. As the temperature is increased, the rate decreases to $\sim 10^{-4}$ of the collision rate at 700 K. Jarrold concludes that the molecularly adsorbed NH_3 state is not stable at high temperatures, and instead they are observing a much less efficient dissociative chemisorption process. For this process, there is substantial variation in rate with cluster size, with Si_{45}^+, Si_{37}^+, and Si_{33}^+ being especially unreactive. Note that both the Bell Labs and Rice groups find 45 and 33 atom clusters unreactive; however, Si_{39}^+ is unreactive in Texas, while Si_{37}^+ is unreactive in New Jersey.

A major complication in understanding silicon cluster ion chemistry is the presence of multiple isomers in the reactant distribution. As discussed above, both the Bell Labs[12] and Rice[66] groups have found evidence for multiple isomers and have studied the effects of laser or collisional annealing on chemical reactivity. Recently Jarrold and Bower[119] have been able to use their drift-tube reactor to separate each isomer and study its chemical properties. The experiment was done using a modified drift cell that can operate at pressures up to 10 Torr. Under these conditions, it is possible to separate isomers that have sufficiently different shapes, taking advantage of the differences in mobility through the buffer gas. Figure 15 shows the results, plotted as relative mobility (measured mobility divided by the estimated hard sphere mobility). For cluster sizes up to 24 atoms, only a single isomer is resolved, which is proposed to have a "sausage" shape, on the basis of the rapid decrease in mobility with increasing size. For Si_{24-34}^+, in addition to the sausage isomer, a second series is observed that is assigned to an oblate or more spherical geometry, on the basis of its higher mobility. For Si_x^+ ($x > 30$), collisional annealing converts the sausage isomer into the more spherical geometry, suggesting that the latter is more stable.

By adding a reactant to the buffer gas in the drift cell, Jarrold and Bower were able to study the reactivity of each isomer component independently. For C_2H_4 there are often large differences, with the sausage shape being less reactive. As an example, Figure 16 shows the time of arrival distributions for Si_{29}^+ with and without ethylene in the drift tube. In 10 Torr of pure helium the two components of the isomer distribution separate into "sphere" and "sausage" peaks. When 5.5 mTorr of C_2H_4 is added to the buffer gas, the peak corresponding to the more spherical isomer(s) is almost completely reacted away, while of the sausage clusters, almost 40% remain. For O_2, the differences between the sausage and spherical isomers are smaller, and the reactivity ordering depends on size. For Si_x^+ (x = 26, 27, 30) the spherical isomer is more reactive, but for Si_x^+ (x = 25, 28, 29) the sausage shape is more reactive. To complicate matters further, the chemistry results show that for some cluster sizes, there are additional isomers which are not resolved in the mobility studies. In addition, comparison of reactivity of small clusters, where all are "sausages", to that of large clusters, which are all "spheres", suggests that there is no large change in overall reactivity associated with this structural transition.

These experiments provide possible rationalizations for the discrepancies between the Bell Labs and Rice groups. (Real explanations will require further exper-

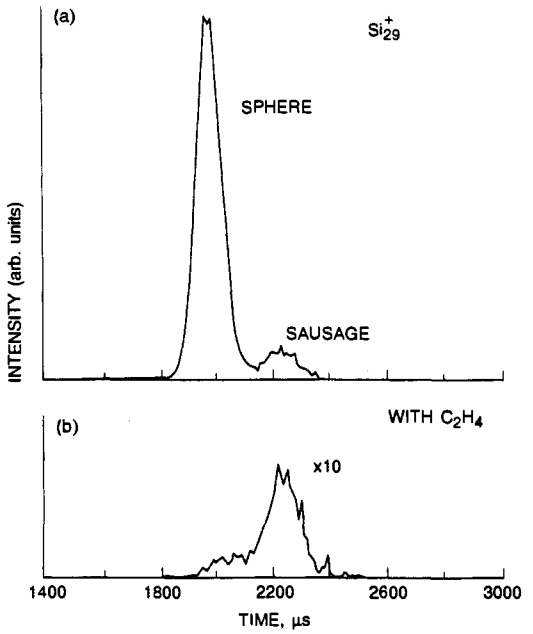

Figure 16. Relative reactivities of different Si_{29}^+ isomers. The top frame shows the arrival time distributions for Si_{29}^+ drifted through 10 Torr of helium. Note separation into peaks consisting of sausage and spherical isomers. The bottom frame shows the result when ~5 mTorr of C_2H_4 is added to the helium in the drift tube. The "spherical" clusters have nearly all reacted away, while the sausage peak is reduced to a much smaller degree. (Reprinted from ref 119. Copyright 1992 American Institute of Physics.)

imental or theoretical work.) One possibility is that the two groups are simply measuring different aspects of the chemistry. The room temperature Bell experiments are done at high enough pressures to allow equilibrium to be established between free and adsorbed ammonia. Under these conditions, all clusters have a high rate for ammonia uptake. The Rice experiments are done at much lower pressures, where the rate of stabilizing collisions is orders of magnitude slower. It may well be that in the Rice experiments, ammonia is molecularly adsorbing with high efficiency, but that the $Si_xNH_3^+$ adduct is rarely stabilized and detected. This would account for the much lower reaction efficiency observed at Rice and could also explain the strong size effects if the adduct binding energies (and thus the lifetimes) are strongly size dependent.

Other rationalizations are also possible. For example, the Bell experiments show that the efficiency of the molecular adsorption process is highly temperature dependent. If the Rice experiments do not completely thermalize the reactant clusters, this could explain their observation of reaction rates well below the collision rate, and it would be most helpful if the Rice group had accurate absolute rate measurements. Temperature arguments do not explain the disagreements regarding which cluster sizes are unreactive. It is conceivable that the cluster sources used in the two groups produce significantly different isomer distributions. In this regard, Smalley has suggested that their cluster source is hotter and quickly builds up clusters atom by atom, while Jarrold's source is colder and builds clusters slowly by aggregation of small clusters. Another difference may be found in the annealing procedure, which may or may not be efficient in converting clusters to the most stable geometry. Isomer effects might explain the discrepancies, particularly if the thermalization/annealing process is size dependent.

IV. Transition Metal Clusters

In contrast to the main group clusters, where the research has been concentrated on boron, aluminum, carbon, and silicon, the studies of transition metal cluster ion chemistry are spread more thinly over a wide range of systems, with less overlap. For this reason it is more difficult to make comparisons and discern trends in the chemistry. Instead of attempting a comprehensive discussion of all the work on transition metal clusters, we will focus on a few selected topics where some comparisons can be made. A summary of the transition metal cluster chemistry literature over the period of this review is given in Table II.

A. Reactions with Hydrogen

Hydrogen (deuterium) is the most commonly used neutral reactant in studies of transition metal cluster ion chemistry. This may be partly due to the precedent set by the pioneering work of Riley and co-workers on neutral transition metal clusters.[120,121] Since hydrogen is a homonuclear diatomic molecule and H-atoms have relatively simple chemistry, this system is a logical prototype for more complex reactions. In the struggle to separate the effects of cluster electronic and geometric structure on reactivity, hydrogen has made an important contribution. The experiments of Cox and co-workers at Exxon, and of Smalley and co-workers at Rice University, will be used as examples.

Cox and co-workers have taken an approach which consists of studying the dependence of reaction kinetics on charge state. Both neutral and charged niobium[17] and iron[16] clusters have been studied in a fast-flow reactor. The reactivity ratios γ^- and γ^+ (defined as the reactivity of the ion $M_x^\pm$ divided by that of the corresponding neutral) are plotted as a function of size for niobium and iron in Figure 17. There is clearly a greater effect of charge on reactivity (either enhancement or inhibition) in the case of iron clusters (Figure 17b), where most of the γ values fall outside the 0.4–2.5 range (i.e. the ion reactivity is more than a factor of 2.5 different from the neutral value). In contrast, most of the niobium cluster ions have a reactivity which is within a factor of 2.5 of the neutral value (the γ points fall within the dashed lines in Figure 17a).

The variation in γ^+ for iron was rationalized by using the frontier orbital model of hydrogen activation.[16] This is a purely electrostatic model with no structural information. Briefly, charge donation from hydrogen to the cluster dominates for small clusters and enhances the reactivity of the cation (x = 4,5). As the cluster increases in size, charge donation from the cluster to the hydrogen becomes more important, with the consequential inhibition in cation reactivity (x = 6–10). For larger clusters, the ion-induced dipole coupling predominates and the cation again becomes more reactive ($x > 10$). The two deviations from the curve are the trimer and x = 18 cations which, respectively, exhibit much lower and higher reactivity than expected. For the trimer this may be due to its small size which is more sensitive to changes in electronic or geometric structure upon ionization. The spike in γ^+ at x = 18

Table II. Summary of Transition Metal Cluster Ion Chemistry Studies*

cluster	neutral†	experiment‡ apparatus	source	refs
V_x^+ (x = 2–7)	C_6H_6	FT-ICR	SIMS	126
V_x^+ (x = 2–19)	C_6H_6	FFR	LV	127
Nb_x^+ (x = 2–15)	C_6H_6	FFR	LV	128
Nb_x^+ (x = 2–27), Nb_x^- (x = 4–27)	D_2	FFR	LV	17
Nb_x^+ (x = 3–25)	H_2	FT-ICR	LV	122
Nb_x^+ (x = 2, 3)	O_2	IB	LV	*a*
Nb_x^+ (x = 2–6)	O_2	ZAB/DT	LV	*b*
$Mo_xO_y^+$ (x = 2–4, y = 4–11)	CID	FT-ICR	DLV, FAB	42
$(MoO_3)_x^-$, $(WO_3)_x^-$ (x = 2–7)	O, S compounds	TQMS	TD, EI	*c*
Fe_x^+ (x = 2, 3)	O_2	IB	LV	*a*
Fe_x^+ (x = 2–31)	D_2	FFR	LV	16
Fe_x^+ (x = 2–13)	NH_3, N_2H_4, C_2H_4, c-C_3H_6	FT-ICR	SIMS	126, 130, 131, 132
FeM^+ (M = Mg, Sc, Nb), $FeLa^{2+}$	hydrocarbons	FT-ICR	DLV	*d, e, f, g*
Co_x^+ (x = 3–10)	C_2H_4, C_6H_6	FT-ICR	SIMS	126
Co_x^+ (x = 2–22)	H_2, CH_4, C_2H_4, C_2H_2, N_2	FFR	LV	124
$Co_xV_y^+$ (x = 2–19, y = 0–2)	H_2	FFR	LV	125
Co_x^+ (x = 2–4), $Co_4(CO)_y^+$ (y = 1–12)	c-C_6H_{12}	FT-ICR	EI	*h*
Co_xNO^+, $Co_xO_y^+$ (x = 2–4, y = 1–4)	O_2, H_2O	FT-ICR	EI	*i, j*
Rh_x^+ (x = 2–54)	D_2	FFR	LV	*k*
Ir_x^+ (x = 2–4), $Ir_4(CO)_y^+$ (y = 1–12)	c-C_6H_{12}	FT-ICR	EI	*h, l*
Ni_x^+ (x = 2–20)	CH_4, C_2H_4, C_6H_6	FT-ICR	SIMS	133, 126
Ni_x^+ (x = 3–54)	D_2	FFR	LV	*k*
Ni_x^+ (x = 2–18)	CID	IB	LV	*m*
Pd_x^+ (x = 2–9)	D_2, C_2H_4	FT-ICR	SIMS	130
Pt_x^+ (x = 2–60)	D_2	FFR	LV	*k*
Cu_x^+ (x = 3–9)	O_2	FT-ICR	SIMS	*n*
Cu_x^+ (x = 2–14)	CO	flow tube	LV	*o*
Cu_x^+ (x = 2, 3)	CT	FT-ICR	DLV	*p*
Cu_x^+ (x = 2–8)	CID	TOF	SIMS	*q*
$Cu_xAg_y^+$ (x, y = 1, 2)	CT	FT-ICR	DLV	*p*
Cu_xCO^+ (x = 6–24)	CID	FT-ICR	LV	*r*
$Cu_xO_y^+$ (x = 2–14, y = 0–8), $Cu_xO_y^-$ (x = 2–21, y = 0–12)	CID	FT-ICR	DLV	43
Ag_x^+ (x = 3–21)	NH_3, C_6H_6	FT-ICR	SIMS	126
Ag_x^+ (x = 2–5)	20 neutrals	FT-ICR	FAB	129
Ag_x^+ (x = 3, 5)	CT	FT-ICR	DLV	*s*
Ag_x^+ (x = 2–5)	CT	FT-ICR	DLV	*p*
Au_x^+ (x = 3–21)	NH_3, C_6H_6	FT-ICR	SIMS	126
Au_x^+ (x = 2–26)	D_2	FFR	LV	*t*
Au_x^+ (x = 2–5)	CT	FT-ICR	DLV	*p*
Au_x^{2+} (x = 2–5), Au_4^{3+}	CT, CID	TQMS	LMIS	*u, v*
Zn_2^+	CT	FT-ICR	DLV	*s*

* Some low-energy CID studies are also listed. † CT = charge transfer studies were performed with various neutrals. ‡ Entries in this column consist of two codes for the experimental apparatus and the cluster source. Apparatus codes: DT, drift tube; FFR, fast-flow reactor; FT-ICR, Fourier transform ion cyclotron resonance mass spectrometer; IB, ion beam; TOF, time-of-flight mass spectrometer; TQMS, triple quadrupole mass spectrometer; ZAB, reverse geometry (BE) mass spectrometer. Source codes: DLV, direct laser vaporization; EI, electron impact; FAB, fast-atom bombardment source; LMIS, liquid–metal ion source; LV, laser vaporization; SIMS, ion sputtering source; TD, thermal desorption. [a] Loh, S. K.; Lian, L.; Armentrout, P. B. *J. Chem. Phys.* **1989**, *91*, 6148. [b] Radi, P. P.; von Helden, G.; Hsu, M.-T.; Kemper, P. R.; Bowers, M. T. *Int. J. Mass Spectrom. Ion Processes* **1991**, *109*, 49. [c] Maleknia, S.; Brodbelt, J.; Pope, K. *J. Am. Soc. Mass Spectrom.* **1991**, *2*, 212. [d] Roth, L. M.; Freiser, B. S.; Bauschlicher, C. W., Jr.; Partridge, H.; Langhoff, S. R. *J. Am. Chem. Soc.* **1991**, *113*, 3274. [e] Lech, L. M.; Gord, J. R.; Freiser, B. S. *J. Am. Chem. Soc.* **1989**, *111*, 8588. [f] Buckner, S. W.; Freiser, B. S. *J. Phys. Chem.* **1989**, *93*, 3667. [g] Huang, Y.; Freiser, B. S. *J. Am. Chem. Soc.* **1988**, *110*, 4434. [h] Pan, Y. H.; Sohlberg, K.; Ridge, D. P. *J. Am. Chem. Soc.* **1991**, *113*, 2406. [i] Klaassen, J. J.; Jacobsen, D. B. *J. Am. Chem. Soc.* **1988**, *110*, 974. [j] Klaassen, J. J.; Jacobsen, D. B. *Inorg. Chem.* **1989**, *28*, 2022. [k] Cox, D. M.; Fayet, P.; Brickman, R.; Hahn, M. Y.; Kaldor, A. *Catal. Lett.* **1990**, *4*, 271. [l] Pan, Y. H.; Ridge, D. P. *J. Phys. Chem.* **1989**, *93*, 3375. [m] Lian, L.; Su, C.-X.; Armentrout, P. B. *J. Chem. Phys.* **1992**, *96*, 7542. [n] Irion, M. P.; Selinger, A. *Chem. Phys. Lett.* **1989**, *158*, 145. [o] Leuchter, R. E.; Harms, A. C.; Castleman, A. W., Jr. *J. Chem. Phys.* **1990**, *92*, 6527. [p] Cheeseman, M. A.; Eyler, J. R. *J. Phys. Chem.* **1992**, *96*, 1082. [q] Begemann, W.; Hecktor, R.; Lui, Y. Y.; Tiggesbäumker, J.; Meiwes-Broer, K. H.; Lutz, H. O. *Z. Phys. D.* **1989**, *12*, 229. [r] Nygren, M. A.; Siegbahn, P. E. M.; Jin, C.; Guo, T.; Smalley, R. E. *J. Chem. Phys.* **1991**, *95*, 6181. [s] Buckner, S. W.; Gord, J. R.; Freiser, B. S. *J. Chem. Phys.* **1988**, *88*, 3678. [t] Cox, D. M.; Brickman, R.; Creegan, K.; Kaldor, A. *Z. Phys. D.* **1991**, *19*, 353. [u] Saunders, W. A. *Phys. Rev. Lett.* **1989**, *62*, 1037. [v] Saunders, W. A.; Fedrigo, S. *Chem. Phys. Lett.* **1989**, *156*, 14.

may be indicative of a major structural change occurring between 17 and 18.

The niobium cluster results depend very little on charge state (+, O, −) and yet show strong deviations in the range $7 \leq x \leq 16$. In this intermediate size range the cluster valence electronic structure may be an important factor. Some other results suggest an alternative explanation, however.[17] Isomers of differing reactivity were noted for Nb_9, Nb_{12}, and Nb_{12}^+. Also the maximum uptake of D_2 molecules per cluster was independent of charge state but highly dependent on cluster size (at least for x = 5–12). These results suggest that geometric structure is the most important factor in determining the reactivity of niobium clusters. The role of electrostatic factors is diminished in niobium clusters (in comparison to iron clusters) because the valence orbitals are more diffuse and thus the electron density is more delocalized.

Elkind et al.[122] have also studied H_2 chemisorption on niobium cluster cations in the FT-ICR, measuring

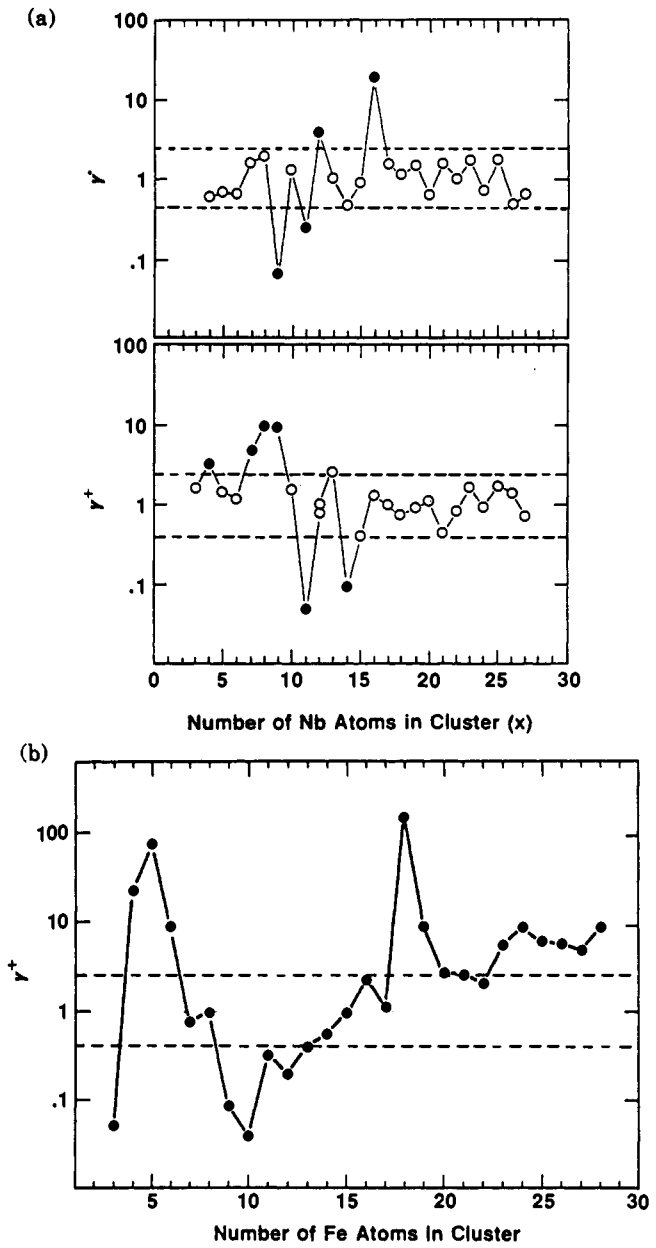

Figure 17. (a) Reactivity ratios γ^- (anion/neutral) and γ^+ (cation/neutral) for niobium clusters reacting with D_2 are plotted as a function of cluster size. The horizontal dashed lines indicate the range of γ for which the ion reactivity is within a factor of 2.5 of the neutral reactivity. The filled points highlight those clusters which fall outside this range. (Adapted and reprinted from ref 17. Copyright 1988 American Institute of Physics.) (b) The reactivity ratio γ^+ (cation/neutral) for iron clusters reacting with D_2 is plotted as a function of cluster size. The horizontal dashed lines indicate the range of γ for which the ion reactivity is within a factor of 2.5 of the neutral reactivity. (Adapted and reprinted from ref 16. Copyright 1988 American Institute of Physics.)

absolute reaction rate constants and H_2 saturation values. The variations with size that they have observed are generally in good qualitative agreement with the results of the Exxon group. Differences were observed in isomer formation, however. In the FT-ICR experiments both Nb_{11}^+ and Nb_{19}^+ have isomers which were differentiated on the basis of reactivity. For example, two different end products were observed for Nb_{11}^+ reacting with H_2, i.e. $Nb_{11}H_6^+$ and $Nb_{11}H_{16}^+$. For Nb_{12}^+ only one form was observed, apparently corresponding to the unreactive isomer produced in the fast-flow reactor. Elkind et al. argue that the observed charge independence of the reactivity, along with the significant changes associated with different structures for clusters of the same size and charge, indicate that geometric factors, including overall structure and active sites, are the most important in determining chemical behavior.

The Rice group further suggests that instead of concentrating on the details of the mechanism of H_2 dissociative chemisorption on active sites, it may be more productive to concentrate on the inert clusters, which contain unreactive sites and presumably have the most symmetrical structures. The FT-ICR is ideally suited for these studies since long ion-trapping times and mass selection can be used to isolate the isomers. In a later study,[123] the Rice group has been able to partially convert the reactive form of Nb_{19}^+ into the unreactive form through laser annealing, discussed earlier for silicon clusters.

The reactions of cobalt cluster cations with hydrogen and several small hydrocarbons have been studied by Nakajima et al. in a fast-flow reactor very similar to that used by the Exxon group. The relative reactivity with H_2 is strongly peaked for clusters containing 13–17 atoms, with a local maximum at $x = 5$.[124] Substituting one vanadium atom for a cobalt atom in the cluster ion enhances the reactivity of the smaller, and generally less reactive, clusters ($x \leq 12$) but inhibits the reactivity of the larger ($x \geq 13$) clusters.[125] The enhancement is particularly strong for the 4 and 5 atom clusters. Substituting a second vanadium for cobalt either has no effect or more commonly, increases reactivity except in the case of $x = 4,5$ for which reactivity decreases (but is still enhanced relative to the pure cobalt cluster). The change in behavior at $x = 13$ is attributed to formation of a geometric structure with an interior position, which is occupied by the V atom. With two V atoms, one must be on the surface where reaction is more favorable than at the Co atom. Similar behavior for the neutral $Co_{x-y}V_y$ clusters also supports an explanation based on geometric structure rather than electronic factors.

B. Reactions with Benzene

Irion and co-workers have looked at the reaction of a variety of small transition metal clusters with benzene in the FT-ICR. Vanadium clusters with 2–7 atoms are very reactive, dehydrogenating benzene to a progressively greater extent as the cluster size is increased.[126] The reaction is very specific, with only one product being observed for each reactant cluster. Clusters with 5–7 atoms completely dehydrogenate the benzene, forming $V_xC_6^+$. Reaction with a second benzene is also specific but the trend is less clear-cut. The dimer, trimer, and hexamer all eliminate H_2 while the heptamer eliminates two H_2, but the tetramer and pentamer only form the adduct. Zakin et al.[127] have also looked at this reaction in the fast-flow reactor. They observe the same trends but the detailed results are different. The extent of dehydrogenation increases with increasing cluster size for the smaller ($x < 13$) clusters; however, they also observe several products for the different size clusters. Total dehydrogenation of the benzene is observed for the 5–7 atom clusters, in agreement with Irion et al., but it is only a minor channel.

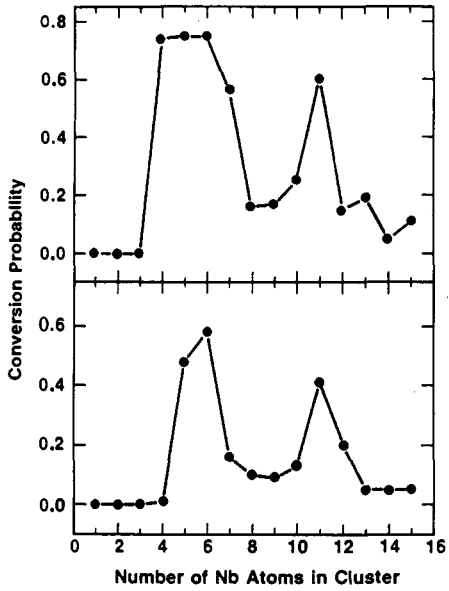

Figure 18. The probability for the reaction of Nb_x^+ (upper panel) and Nb_x (lower panel) with benzene to yield the completely dehydrogenated product $Nb_xC_6^+$ or Nb_xC_6 is plotted as a function of niobium cluster size. (Adapted and reprinted from ref 128. Copyright 1988 American Institute of Physics.)

These differences in reactivity may be due to the different pressure regimes of the two experiments. In the high-pressure fast-flow reactor, dehydrogenation may be occurring but collisions stabilize the product so that the hydrogens remain bound to the cluster. This idea is supported by work on the neutral clusters where hydrogen loss is observed when the ionizing photon energy is increased. Another possibility is that the ions in the two experiments have different internal energy content: in studies of niobium clusters, increasing the cluster energy increased the rate, but not the extent, of dehydrogenation.[128] The cluster ions in the FT-ICR do undergo thermalizing collisions before reaction; however, it is possible that the reaction is very sensitive to even small amounts of internal energy. Lack of information on these points makes it impossible to definitively explain the observed discrepancies.

The Exxon group[128] has also studied the dehydrogenation of benzene by niobium cluster cations. There is an interesting "duality" in the results: for clusters containing less than 4 atoms, H_2 is eliminated, while clusters with 4 or more atoms completely dehydrogenate the benzene. The partial dehydrogenation products were not observed under any of the conditions utilized. The results are very similar to what had been previously observed for neutral niobium clusters reacting with benzene as shown in Figure 18, suggesting that geometric factors are the most important. One major difference between the neutral and cation cluster reactivity is the minimum size cluster required for complete dehydrogenation to occur: it is 4 for the cations but 5 for the neutral clusters. It is also 5 for the monooxide species Nb_xO^+, thus the active site may be four niobium atoms with a net positive charge.

Vanadium and niobium are both group 5 metals, but they have different electronic configurations: V is a d^3s^2 metal while Nb is a d^4s^1 metal. The higher reactivity of niobium compared to vanadium may be due to this difference in electronic structure. Another explanation arises from the fact that the d orbitals of niobium are much larger than those of vanadium, making them more accessible for chemical interaction. Tantalum would be an interesting case study since it has a d^3s^2 configuration like vanadium, but is about the same size as niobium.

Irion et al.[126] have also studied the reactions of small cobalt, nickel, silver, and gold cluster cations with benzene. Cobalt, silver, and gold clusters reversibly add 1 to 3 benzenes, with no evidence of any dehydrogenation. This behavior is similar to that documented in another study of silver cluster cations containing 2–5 atoms, in which adduct formation was the only observed reaction pathway.[129] Nickel cations present the most varied chemical behavior of all the systems studied. The dimer is unreactive while the $x = 3$ and 4 clusters add 2 or 3 benzenes respectively. Dehydrogenation is first observed for the $x = 5$ and 6 clusters, as shown:

$$Ni_{5,6}^+ \rightarrow Ni_{5,6}X^+ \rightarrow Ni_{5,6}XY^+ \rightarrow Ni_{5,6}X_2Y^+ \rightarrow Ni_{5,6}XY_3^+ \rightarrow Ni_5XY_4^+$$

where $X = C_6H_6$ and $Y = C_6H_4$. Two unique processes are observed in this reaction sequence: the first is dehydrogenation which only occurs after one benzene has been adsorbed; the second is the fourth step which involves either the double dehydrogenation of one benzene or the coordinated single dehydrogenation of two benzenes. Experiments using a mixture of C_6H_6 and C_6D_6 should be able to resolve this question.

In this survey of benzene reactions, we have seen that reactivity (defined as the ability to dehydrogenate benzene) decreases as one moves across the periodic table from early to late transition metals. One exception is the Co/Ni pair: cobalt clusters were all unreactive while nickel clusters with 5 or 6 atoms were quite reactive. Do these nickel clusters represent an anomaly? Reactivity studies with other group 9 and 10 metals as well as iron might be useful in determining the important factors governing benzene dehydrogenation.

C. The Special Nature of the Tetramer and Pentamer Clusters

A number of studies have remarked on the relatively high reactivity of transition metal clusters containing 4 or 5 atoms. As discussed above, the smallest vanadium or niobium cluster which can dehydrogenate benzene in the fast-flow reactor is the tetramer.[127,128] (Caveat: In the FT-ICR the vanadium dimer and trimer cations also dehydrogenated benzene.)

Iron cluster cations have been reacted with a variety of small neutrals.[126,130,131] Fe_4^+ is certainly one of the most interesting transition metal clusters. The small iron cluster cations generally react with ammonia by adduct formation. The exception is the tetramer, which rapidly reacts via the following sequence:

$$Fe_4^+ \rightarrow Fe_4(NH)^+ \rightarrow Fe_4(NH)_2^+ \rightarrow Fe_3(NH)_2(NH_3)^+ \rightarrow Fe_3(NH)_2(NH_3)_2^+$$

$$Fe_4(NH)_2(NH_3)^+ \rightarrow Fe_4(NH)_2(NH_3)_2^+$$

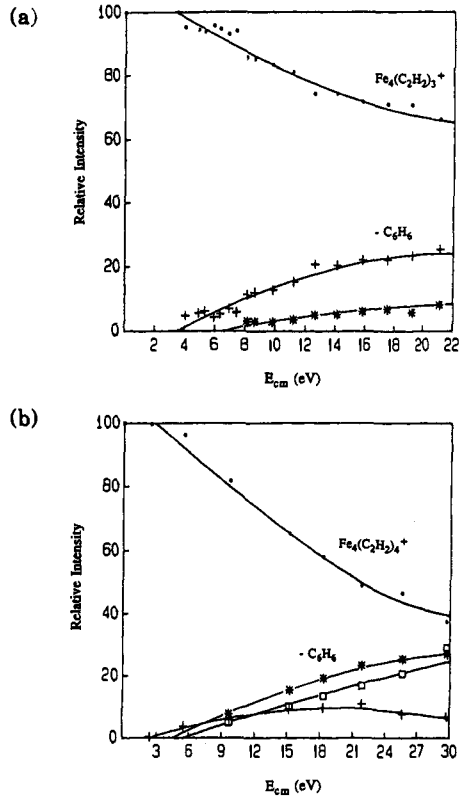

Figure 19. Relative ion intensities for the CID of $Fe_4(C_2H_2)_3^+$ (top panel) and $Fe_4(C_2H_2)_4^+$ (bottom panel) as a function of collision energy. The first two fragment ions observed from $Fe_4(C_2H_2)_3^+$ are Fe_4^+ (+) and $Fe_4C_4H_2^+$ (*). The fragment ions observed from $Fe_4(C_2H_2)_4^+$ are $Fe_4(C_2H_2)_3^+$ (+), $Fe_4(C_2H_2)^+$ (*), and Fe_4^+ (□). (Adapted and reprinted from ref 132. Copyright 1991 American Chemical Society.)

The products containing three iron atoms cannot be obtained starting directly from Fe_3^+.

In reactions with ethylene and cyclopropane, the reactive iron clusters were x = 4,5 and x = 3–5, respectively.[132] The chemistry, especially with cyclopropane, is quite complex and will not be discussed in detail here. Instead, we will focus on one product of the tetramer reactions. With both neutrals, Fe_4^+ forms products of stoichiometry $Fe_4C_6H_6^+$. CID of these ions and other ions in the same reaction path indicate that the C_6H_6 moiety is weakly bound and easily removed, as seen in Figure 19, leading to the conclusion that benzene is being detached. If this is indeed the case, then this work represents the first catalytic synthesis of a molecule from smaller components on a cluster. (A similar product was observed for the pentamer ion reacting with cyclopropane but unfortunately it was not studied in further detail.)

The cobalt tetramer and pentamer are the most reactive of the small cluster cations of these elements,[126] dehydrogenating 5 and 3 ethylenes, respectively. Nakajima et al.[124] have measured the chemisorption reaction rate constants of cobalt cluster cations with several neutrals and observe a local maximum in the rate constant at x = 5. In addition they note that Co_4^+ and Co_5^+ are particularly reactive when compared to the neutral clusters. The same group has also shown that these two clusters exhibit an unusually large enhancement in reactivity toward H_2 when a V atom is substituted for a Co atom.[125] In the reactions of nickel cluster cations with benzene and ethylene, dehydrogenation products are observed for the pentamer and larger clusters but not for the tetramer.[126,133]

Nakajima et al.[124] have taken similarity of these results as evidence for the dominance of cluster geometry over electronic effects in determining reactivity for this size range. Irion and Schnabel[131] have also discussed the enhanced reactivity of metal tetramers. In their view, the onset of reactivity at x = 4 or 5 is correlated to the transition from a nonreactive planar structure to a reactive three-dimensional one.

V. Final Thoughts

We hope that this review has given the flavor (if not the substance) of the progress that has been made in the past few years toward understanding the chemistry of metal and semimetal cluster ions. For boron, aluminum, carbon, and silicon there are copious results, both theoretical and experimental, which bear on the cluster geometric and electronic structures, and their relationship to chemical reactivity. For carbon, this has led to a qualitative understanding of the structure–chemistry relationship, at least for small cluster ions. The roles of isomerism, dangling bonds, ring strain, and other familiar chemical concepts have been explored. Much of the activity in this area is now directed at understanding fullerene chemistry. For other main group elements the situation is promising, but not nearly so well understood. For example, results on silicon cluster ion chemistry from different techniques are qualitatively inconsistent, and experiments have just begun to reveal some of the complexities that underlie this problem.

Despite the strong motivation to understand transition metal cluster ion chemistry, with its potential connection to heterogeneous catalysis, there are two factors that have resulted in an incomplete picture. First, the experimental results are spread more thinly over a large number of metal–molecule systems, thus affording fewer opportunities to compare results. In addition, these systems are very difficult to attack theoretically, and little ab initio information is available on electronic or geometric structures. Transition metal cluster chemistry has not benefited from the close interplay of experiment and theory that has been so helpful in understanding small main group clusters.

We have seen that evidence for isomeric forms of clusters has been obtained in several experiments. Yet isomers are far from ubiquitous, even though one might expect all clusters containing more than a few atoms to possess different isomeric structures. There are several possible explanations for this situation. First we need to consider if isomers are indeed present. If the differences in energy between different isomers are large enough, the most stable structure will be the only one produced. In fact the energy difference needed, such that 10% of the cluster population is in the higher energy state, is not very large at all, being on the order of a few kilocalories per mole or less. For experiments in which the clusters have been efficiently annealed, most likely only one isomer will be present. In many experiments however, the clusters can easily have enough internal energy to populate several isomeric states. Isomers might not be differentiated if the chemical reactivity of the isomers is not sufficiently distinct to be measured in the typical cluster chemistry

experiment. The chemistry itself may change the isomer distribution. For most systems (metals), the bonds between the metal atom in the cluster and a heteroatom in the chemical probe are stronger and more directional than the metal–metal bonds in the cluster itself. Exposing the cluster isomer distribution to a reactant can chemically anneal the clusters to the most stable product structure. In this light, when isomers *are* observed they signal significant differences, a special structure.

There are a number of areas which seem to us to be fruitful avenues for further work. Mixed clusters (e.g. the N-terminated carbon cluster ions) may offer a means to chemically label or block particular sites on the cluster. This can be a potentially useful tool for qualitative structure elucidation and may provide insight into reaction mechanisms. Separating and studying the chemistry of structural isomers is another important problem; it has only been seriously addressed for carbon and very recently attacked in the case of silicon. Given that different isomers may have very different reactivities, this is a critical issue in understanding cluster chemistry. In the theoretical realm, the most pressing need is for very accurate calculations on the systems where these are feasible. Ideally, these calculations would tell us not only what the ground state is, but also the energetics and structures of isomeric states. As alluded to above, development of methods to treat transition metal clusters is also an important problem. Finally, the calculation of cluster dynamics, using approximate potential energy surfaces, is another area that merits further exploration.

Acknowledgments. The cluster program at the Naval Research Laboratory is funded by the Office of Naval Research. S.L.A. gratefully acknowledges support from a Camille and Henry Dreyfus Foundation Teacher–Scholar Fellowship. Cluster work at Stony Brook is supported by the Office of Naval Research (Mechanics Division) under grant no. N0001492J1202.

VI. Bibliography

(1) Jarrold, M. F. In *Gas Phase Inorganic Chemistry*; Russell, D. H., Ed.; Plenum Press: New York, 1989; pp 137–92.
(2) Buckner, S. W.; Freiser, B. S. In *Gas Phase Inorganic Chemistry*; Russell, D. H., Ed.; Plenum Press: New York, 1989; pp 279–322.
(3) Mandich, M. L. In *The Chemical Physics of Atomic and Molecular Clusters*; Scoles, G., Ed.; North-Holland: Amsterdam, 1990; pp 635–760.
(4) Mandich, M. L.; Reents, W. D., Jr.; Bondybey, V. E. In *Atomic and Molecular Clusters*; Bernstein, E. R., Ed.; Elsevier: Amsterdam, 1990; pp 69–357.
(5) McElvany, S. W.; Ross, M. M. *J. Am. Soc. Mass Spectrom.* **1992**, *3*, 268.
(6) McElvany, S. W.; Ross, M. M.; Callahan, J. H. *Acc. Chem. Res.* **1992**, *25*, 162.
(7) Ferguson, E. E.; Fehsenfeld, F. C.; Schmeltekopf, A. L. *Adv. At. Mol. Phys.* **1969**, *5*, 1.
(8) McFarland, M.; Albritton, D. L.; Fehsenfeld, F. C.; Ferguson, E. E.; Schmeltekopf, A. L. *J. Chem. Phys.* **1973**, *59*, 6610.
(9) Adams, N. G.; Smith, D. *Int. J. Mass Spectrom. Ion Phys.* **1976**, *21*, 349.
(10) Smith, D.; Adams, N. G. In *Gas Phase Ion Chemistry*; Bowers, M. T., Ed.; Academic: New York, 1979; Vol. 1, pp 1–44.
(11) Kemper, P. R.; Bowers, M. T. *J. Am. Soc. Mass Spectrom.* **1990**, *1*, 197.
(12) Jarrold, M. F.; Bower, J. E.; Creegan, K. *J. Chem. Phys.* **1989**, *90*, 3615.
(13) (a) Geusic, M. E.; Morse, M. D.; O'Brien, S. C.; Smalley, R. E. *Rev. Sci. Instr.* **1985**, *56*, 2123. (b) Morse, M. D.; Geusic, M. E.; Heath, J. R.; Smalley, R. E. *J. Chem. Phys.* **1985**, *83*, 2293.
(14) Whetten, R. L.; Cox, D. M.; Trevor, D. J.; Kaldor, A. *J. Phys. Chem.* **1985**, *89*, 566.
(15) Nonose, S.; Sone, Y.; Onodera, K.; Sudo, S.; Kaya, K. *J. Phys. Chem.* **1990**, *94*, 2744.
(16) Zakin, M. R.; Brickman, R. O.; Cox, D. M.; Kaldor, A. *J. Chem. Phys.* **1988**, *88*, 6605.
(17) Zakin, M. R.; Brickman, R. O.; Cox, D. M.; Kaldor, A. *J. Chem. Phys.* **1988**, *88*, 3555.
(18) Beauchamp, J. L. In *Annual Review of Physical Chemistry*; Eyring, H., Christensen, C. J., Johnston, H. S., Eds.; Annual Reviews Inc.: Palo Alto, 1971; Vol. 22, pp 527–561.
(19) Wanczek, K. P. *Int. J. Mass Spectrom. Ion Processes* **1984**, *60*, 11.
(20) Comisarow, M. *Adv. Mass Spectrom.* **1978**, *7*, 1042.
(21) Comisarow, M. B. In *Transform Techniques in Chemistry*; Griffiths, P. R., Ed.; Plenum: New York, 1978; pp 257–284.
(22) Gross, M. L.; Rempel, D. L. *Science (Washington, D.C.)* **1984**, *226*, 261.
(23) Marshall, A. G. *Acc. Chem. Res.* **1985**, *18*, 316.
(24) Comisarow, M. B. *Anal. Chim. Acta* **1985**, *178*, 1.
(25) Marshall, A. G.; Wang, T. C. L.; Ricca, T. L. *J. Am. Chem. Soc.* **1985**, *107*, 7893.
(26) Alford, J. M.; Laaksonen, R. T.; Smalley, R. E. *J. Chem. Phys.* **1991**, *94*, 2618.
(27) Futrell, J. H. In *Gaseous Ion Chemistry and Mass Spectrometry*; Futrell, J. H., Ed.; Wiley: New York, 1986; pp 201–236.
(28) Farrar, J. M. In *Techniques for the Study of Ion-Molecule Reactions*; Farrar, J. M., Saunders, W. H., Jr.; Eds.; Wiley: New York, 1988; pp 325–416.
(29) Hales, D. A.; Li, L.; Armentrout, P. B. *Int. J. Mass Spectrom. Ion Processes* **1990**, *102*, 269.
(30) Wan, Z.; Christian, J. F.; Anderson, S. L. *J. Chem. Phys.* **1992**, *96*, 3344.
(31) Hanley, L.; Ruatta, S. A.; Anderson, S. L. *J. Chem. Phys.* **1987**, *87*, 260.
(32) Gerlich, D. In *State-Selected and State-to-State Ion-Molecule Reaction Dynamics, Part 1: Experiment*; Ng, C. Y., Baer, M., Eds.; *Adv. Chem. Phys.* 1992; Vol. LXXXII, pp 1–176.
(33) Jarrold, M. F.; Bower, J. E.; Kraus, J. S. *J. Chem. Phys.* **1987**, *86*, 3876.
(34) Loh, S. K.; Hales, D. A.; Li, L.; Armentrout, P. B. *J. Chem. Phys.* **1989**, *90*, 5466.
(35) Christian, J.; Wan, Z.; Anderson, S. L. *Rev. Sci. Instrum.*, in preparation.
(36) McElvany, S. W.; Creasy, W. R.; O'Keefe, A. *J. Chem. Phys.* **1986**, *85*, 632.
(37) Zimmerman, J. A.; Eyler, J. R.; Bach, S. B. H.; McElvany, S. W. *J. Chem. Phys.* **1991**, *94*, 3556.
(38) Mandich, M. L.; Reents, W. D., Jr.; Bondybey, V. E. *J. Phys. Chem.* **1986**, *90*, 2315.
(39) King, F. L.; Dunlap, B. I.; Parent, D. C. *J. Chem. Phys.* **1991**, *94*, 2578.
(40) Parent, D. C. *Chem. Phys. Lett.* **1991**, *183*, 45.
(41) McElvany, S. W.; Cassady, C. J. *J. Phys. Chem.* **1990**, *94*, 2057.
(42) Cassady, C. J.; Weil, D. A.; McElvany, S. W. *J. Chem. Phys.* **1992**, *96*, 691.
(43) Gord, J. R.; Bemish, R. J.; Freiser, B. S. *Int. J. Mass Spectrom. Ion Processes* **1990**, *102*, 115.
(44) Hettich, R. L. *J. Am. Chem. Soc.* **1989**, *111*, 8582.
(45) Bach, S. B. H.; McElvany, S. W.; Wong, N.; Parent, D. C. *Chem. Phys. Lett.*, in preparation.
(46) Parent, D. C.; McElvany, S. W. *J. Am. Chem. Soc.* **1989**, *111*, 2393.
(47) Cassady, C. J.; McElvany, S. W. *J. Am. Chem. Soc.* **1990**, *112*, 4788.
(48) Parent, D. C. *Int. J. Mass Spectrom. Ion Processes* **1992**, *116*, 257.
(49) Hanley, L.; Whitten, J. L.; Anderson, S. L. *J. Phys. Chem.* **1988**, *92*, 5803.
(50) Dietz, T. G.; Duncan, M. A.; Powers, D. E.; Smalley, R. E. *J. Chem. Phys.* **1981**, *74*, 6511.
(51) Jarrold, M. F.; Bower, J. E.; Kraus, J. S. *J. Chem. Phys.* **1987**, *86*, 3876.
(52) Alford, J. M.; Williams, P. E.; Trevor, D. J.; Smalley, R. E. *Int. J. Mass Spectrom. Ion Processes* **1986**, *72*, 33.
(53) Kitsopoulos, T. N.; Chick, C. J.; Weaver, A.; Neumark, D. M. *J. Chem. Phys.* **1990**, *93*, 6108.
(54) LaiHing, K.; Cheng, P. Y.; Duncan, M. A. *Z. Phys. D.* **1989**, *13*, 161.
(55) Morse, M. D. *Chem. Rev.* **1986**, *86*, 1049.
(56) Bucher, J. P.; Douglass, D. C.; Xia, P.; Haynes, B.; Bloomfield, L. A. *Z. Phys. D.* **1991**, *19*, 251.
(57) Kolenbrander, K. D.; Mandich, M. L. *J. Chem. Phys.* **1990**, *92*, 4759.
(58) Wittmaack, K. In *Inelastic Ion-Surface Collisions*; Tolk, N. H., Tully, J. C., Heiland, W., White, C. W., Eds.; Academic Press: New York, 1977; pp 153–199.
(59) Harbich, W.; Fedrigo, S.; Meyer, F.; Lindsay, D. M.; Lignieres, J.; Rivoal, J. C.; Kreisle, D. *J. Chem. Phys.* **1990**, *93*, 8535.
(60) Schnabel, P.; Irion, M. P.; Weil, K. G. *Ber. Bunsen-Ges. Phys. Chem.* **1991**, *95*, 197.
(61) Hanley, L.; Anderson, S. L. *Chem. Phys. Lett.* **1985**, *122*, 410.
(62) Begemann, W.; Meiwes-Broer, K. H.; Lutz, H. O. *Phys. Rev. Lett.* **1986**, *56*, 2248.
(63) Selinger, A.; Schnabel, P.; Weise, W.; Irion, M. P. *Ber. Bunsen-Ges. Phys. Chem.* **1990**, *94*, 1278.
(64) Bach, S. B. H.; Eyler, J. R. *J. Chem. Phys.* **1990**, *92*, 358.

(65) Jarrold, M. F.; Honea, E. C. *J. Am. Chem. Soc.* **1992**, *114*, 459.
(66) Maruyama, S.; Anderson, L. R.; Smalley, R. E. *J. Chem. Phys.* **1990**, *93*, 5349.
(67) *Boron, Metallic-boron Compounds, and Boranes*; Adams, R. M., Ed.; Interscience: New York, 1964.
(68) Muetterties, E. L.; Knoth, W. H. *Polyhedral Boranes*; Dekker: New York, 1968.
(69) Kato, H.; Tanaka, E. *J. Comput. Chem.* **1991**, *12*, 1097.
(70) Kato, H.; Yamashita, K.; Morokuma, K. Private communication.
(71) Bonačić-Koutecký, V.; Fantucci, P.; Koutecký, J. *Chem. Rev.* **1991**, *91*, 1035.
(72) Kawai, R.; Weare, J. H. *J. Chem. Phys.* **1991**, *95*, 1151.
(73) Kawai, R.; Weare, J. H. *Chem. Phys. Lett.* **1992**, *191*, 311.
(74) Hanley, L.; Anderson, S. L. *J. Chem. Phys.* **1988**, *89*, 2848.
(75) Ruatta, S. A.; Hintz, P. A.; Anderson, S. L. *J. Chem. Phys.* **1991**, *94*, 2833.
(76) Hintz, P. A.; Sowa, M. B.; Ruatta, S. A.; Anderson, S. L. *J. Chem. Phys.* **1991**, *94*, 6446.
(77) Hintz, P. A.; Ruatta, S. A.; Anderson, S. L. *J. Chem. Phys.* **1990**, *92*, 292.
(78) Ruatta, S. A.; Hanley, L.; Anderson, S. L. *J. Chem. Phys.* **1989**, *91*, 226.
(79) Hintz, P. A.; Ruatta, S. A.; Sowa, M. B.; Anderson, S. L. *J. Phys. Chem.*, manuscript in preparation.
(80) Weare, J. H. Private communication.
(81) Cotton, F. A.; Wilkinson, G. *Advanced Inorganic Chemistry*, 4th ed.; Wiley: New York, 1980.
(82) Ray, U.; Jarrold, M. F.; Bower, J. E.; Kraus, J. S. *J. Chem. Phys.* **1989**, *91*, 2912.
(83) Upton, T. H. *J. Chem. Phys.* **1987**, *86*, 7054.
(84) Pettersson, L. G. M.; Bauschlicher, C. W., Jr.; Halicioglu, T. *J. Chem. Phys.* **1987**, *87*, 2205.
(85) Jarrold, M. F.; Bower, J. E. *J. Chem. Phys.* **1987**, *87*, 5728.
(86) Jarrold, M. F.; Bower, J. E. *J. Chem. Phys.* **1987**, *87*, 1610.
(87) Ruatta, S. A.; Anderson, S. L. *J. Chem. Phys.* **1988**, *89*, 273.
(88) Leuchtner, R. E.; Harms, A. C.; Castleman, A. W., Jr. *J. Chem. Phys.* **1991**, *94*, 1093.
(89) Drowart, J.; DeMaria, G.; Burns, R. P.; Ingram, M. G. *J. Chem. Phys.* **1960**, *32*, 1366.
(90) Doyle, R. J., Jr. *J. Am. Chem. Soc.* **1988**, *110*, 4120.
(91) Slanina, Z.; Zahradnik, R. *J. Phys. Chem.* **1977**, *81*, 2252.
(92) Ray, A. K. *J. Phys. B.* **1987**, *20*, 5233.
(93) Whiteside, R. A.; Krishnan, R.; Defrees, D. J.; Pople, J. A.; Schleyer, P. v. R. *Chem. Phys. Lett.* **1981**, *78*, 538.
(94) Magers, D. H.; Harrison, R. J.; Bartlett, R. J. *J. Chem. Phys.* **1986**, *84*, 3284.
(95) Rao, B. K.; Khanna, S. N.; Jena, P. *Solid State Commun.* **1986**, *58*, 53.
(96) Raghavachari, K.; Binkley, J. S. *J. Chem. Phys.* **1987**, *87*, 2191.
(97) Bernholdt, D. E.; Magers, D. H.; Bartlett, R. J. *J. Chem. Phys.* **1988**, *89*, 3612.
(98) Bernholc, J.; Phillips, J. C. *J. Chem. Phys.* **1986**, *85*, 3258.
(99) See reviews by Weltner and Van Zee and Heath: Weltner, W., Jr.; Van Zee, R. J. *Chem. Rev.* **1989**, *89*, 1713. Heath, J. R. *Spectroscopy* **1990**, *5*, 36. Also see: Heath, J. R.; Saykally, R. J. *J. Chem. Phys.* **1990**, *93*, 8392; *J. Chem. Phys.* **1991**, *94*, 3271 and references therein.
(100) Bohme, D. K.; Wlodek, S.; Williams, L.; Forte, L.; Fox, A. *J. Chem. Phys.* **1987**, *87*, 6934.
(101) Bohme, D. K.; Dheandhanoo, S.; Wlodek, S.; Raksit, A. B. *J. Phys. Chem.* **1987**, *91*, 2569.
(102) Bohme, D. K.; Wlodek, S.; Raksit, A. B. *Can. J. Chem.* **1987**, *65*, 1563.
(103) Bohme, D. K.; Raksit, A. B.; Fox, A. *J. Am. Chem. Soc.* **1983**, *105*, 5481.
(104) McElvany, S. W.; Dunlap, B. I.; O'Keefe, A. *J. Chem. Phys.* **1987**, *86*, 715.
(105) McElvany, S. W. *J. Chem. Phys.* **1988**, *89*, 2063.
(106) Lifshitz, C.; Peres, T.; Kababia, S.; Agranat, I. *Int. J. Mass Spectrom. Ion Processes* **1988**, *82*, 193.
(107) Hintz, P. A.; Sowa, M. B.; Anderson, S. L. *Chem. Phys. Lett.* **1991**, *177*, 146.
(108) Sowa, M. B.; Hintz, P. A.; Goldman, I.; Anderson, S. L. *J. Chem. Phys.* **1992**, in press.
(109) McElvany, S. W. *Int. J. Mass Spectrom. Ion Processes* **1990**, *102*, 81.
(110) von Helden, G.; Hsu, M.-T.; Kemper, P. R.; Bowers, M. T. *J. Chem. Phys.* **1991**, *95*, 3835.
(111) Bohme, D. K.; Wlodek, S. *Int. J. Mass Spectrom. Ion Processes* **1990**, *102*, 133.
(112) Parent, D. C. *Astrophys. J.* **1989**, *347*, 1183.
(113) Parent, D. C. *J. Am. Chem. Soc.* **1990**, *112*, 5966.
(114) Creasy, W. R.; O'Keefe, A.; McDonald, J. R. *J. Phys. Chem.* **1987**, *91*, 2848.
(115) Parent, D. C. *J. Phys. Chem.* **1992**, submitted for publication.
(116) Maruyama, S.; Anderson, L. R.; Smalley, R. E. *Rev. Sci. Instrum.* **1990**, *61*, 3686.
(117) Anderson, L. R.; Maruyama, S.; Smalley, R. E. *Chem. Phys. Lett.* **1991**, *176*, 348.
(118) Jarrold, M. F.; Ijiri, Y.; Ray, U. *J. Chem. Phys.* **1991**, *94*, 3607.
(119) Jarrold, M. F.; Bower, J. E. *J. Chem. Phys.* **1992**, *96*, 9180.
(120) Richtsmeier, S. C.; Parks, E. K.; Liu, K.; Pobo, L. G.; Riley, S. J. *J. Chem. Phys.* **1985**, *82*, 3659.
(121) Parks, E. K.; Weiller, B. H.; Bechthold, P. S.; Hoffman, W. F.; Nieman, G. C.; Pobo, L. G.; Riley, S. J. *J. Chem. Phys.* **1988**, *88*, 1622.
(122) Elkind, J. L.; Weiss, F. D.; Alford, J. M.; Laaksonen, R. T.; Smalley, R. E. *J. Chem. Phys.* **1988**, *88*, 5215.
(123) Maruyama, S.; Guo, T.; Chen, C.; Laaksonen, R. T.; Smalley, R. E. *Chem. Phys. Lett.* **1991**, submitted for publication.
(124) Nakajima, A.; Kishi, T.; Sone, Y.; Nonose, S.; Kaya, K. *Z. Phys. D.* **1991**, *19*, 385.
(125) Nakajima, A.; Kishi, T.; Sugioka, T.; Sone, Y.; Kaya, K. *J. Phys. Chem.* **1991**, *95*, 6833.
(126) Irion, M. P.; Schnabel, P.; Selinger, A. *Ber. Bunsen-Ges. Phys. Chem.* **1990**, *94*, 1291.
(127) Zakin, M. R.; Cox, D. M.; Brickman, R. O.; Kaldor, A. *J. Phys. Chem.* **1989**, *93*, 6823.
(128) Zakin, M. R.; Brickman, R. O.; Cox, D. M.; Kaldor, A. *J. Chem. Phys.* **1988**, *88*, 5943.
(129) Sharpe, P.; Cassady, C. J. *Chem. Phys. Lett.* **1992**, *191*, 111; **1992**, *197*, 338.
(130) Irion, M. P.; Selinger, A.; Schnabel, P. *Z. Phys. D.* **1991**, *19*, 393.
(131) Irion, M. P.; Schnabel, P. *J. Phys. Chem.* **1991**, *95*, 10596.
(132) Schnabel, P.; Irion, M. P.; Weil, K. G. *J. Phys. Chem.* **1991**, *95*, 9688.
(133) Irion, M. P.; Selinger, A. *Ber. Bunsen-Ges. Phys. Chem.* **1989**, *93*, 1408.